



HAL
open science

The melon Fom-1–Prv resistance gene pair: Correlated spatial expression and interaction with a viral protein

Michael Normantovich, Arie Amitzur, Sharon Offri, Ekaterina Pashkovsky, Yula Shnaider, Shahar Nizan, Ohad Yogev, Avi Jacob, Christopher G. Taylor, Cecile Desbiez, et al.

► To cite this version:

Michael Normantovich, Arie Amitzur, Sharon Offri, Ekaterina Pashkovsky, Yula Shnaider, et al.. The melon Fom-1–Prv resistance gene pair: Correlated spatial expression and interaction with a viral protein. *Plant Direct*, 2024, 8 (2), pp.e565. 10.1002/pld3.565 . hal-04477304

HAL Id: hal-04477304

<https://hal.inrae.fr/hal-04477304>

Submitted on 26 Feb 2024

HAL is a multi-disciplinary open access archive for the deposit and dissemination of scientific research documents, whether they are published or not. The documents may come from teaching and research institutions in France or abroad, or from public or private research centers.





L'archive ouverte pluridisciplinaire **HAL**, est destinée au dépôt et à la diffusion de documents scientifiques de niveau recherche, publiés ou non, émanant des établissements d'enseignement et de recherche français ou étrangers, des laboratoires publics ou privés.



Distributed under a Creative Commons Attribution 4.0 International License

RESEARCH ARTICLE

The melon *Fom-1-Prv* resistance gene pair: Correlated spatial expression and interaction with a viral protein

Michael Normantovich¹  | Arie Amitzur¹ | Sharon Offri¹ |
 Ekaterina Pashkovsky¹ | Yula Shnaider¹ | Shahar Nizan¹ | Ohad Yogev¹ |
 Avi Jacob¹ | Christopher G. Taylor² | Cécile Desbiez³  | Steven A. Whitham⁴  |
 Amalia Bar-Ziv¹ | Rafael Perl-Treves¹ 

¹The Mina and Everard Goodman Faculty of Life Sciences, Bar Ilan University, Ramat Gan, Israel

²Department of Plant Pathology, Ohio State University, Columbus, Ohio, USA

³Plant Pathology Unit, INRA, Montfavet, France

⁴Department of Plant Pathology and Microbiology, Iowa State University, Ames, Iowa, USA

Correspondence

Rafael Perl-Treves, The Mina and Everard Goodman Faculty of Life Sciences, Bar Ilan University, Ramat Gan 5290002, Israel.
 Email: rafi.perl@gmail.com

Funding information

This research was funded in part by ISF grant No. 16/1137 of the Israel Science Foundation.

Abstract

The head-to-head oriented pair of melon resistance genes, *Fom-1* and *Prv*, control resistance to *Fusarium oxysporum* races 0 and 2 and papaya ringspot virus (PRSV), respectively. They encode, via several RNA splice variants, TIR-NBS-LRR proteins, and *Prv* has a C-terminal extra domain with a second NBS homologous sequence. In other systems, paired R-proteins were shown to operate by “labor division,” with one protein having an extra integrated domain that directly binds the pathogen’s Avr factor, and the second protein executing the defense response. We report that the expression of the two genes in two pairs of near-isogenic lines was higher in the resistant isolate and inducible by *F. oxysporum* race 2 but not by PRSV. The intergenic DNA region separating the coding sequences of the two genes acted as a bi-directional promoter and drove GUS expression in transgenic melon roots and transgenic tobacco plants. Expression of both genes was strong in melon root tips, around the root vascular cylinder, and the phloem and xylem parenchyma of tobacco stems and petioles. The pattern of GUS expression suggests coordinated expression of the two genes. In agreement with the above model, *Prv*’s extra domain was shown to interact with the cylindrical inclusion protein of PRSV both in yeast cells and *in planta*.

KEYWORDS

Cucumis melo, cylindrical inclusion protein, *Fom-1*, *Fusarium oxysporum*, integrated decoy, melon, PRSV, *Prv*, R-gene pair

1 | INTRODUCTION

Plants are equipped with dominant resistance (R) genes that provide them with a highly specific surveillance system against diverse

pathogens and pests (Innes, 2004; van Wersch et al., 2020). Most R proteins belong to the nucleotide binding site leucine-rich repeat (NLR) superfamily. NLR proteins trigger a gene-for-gene defense response following recognition of pathogen-encoded effectors or avirulence (Avr) determinants. NLR proteins have been modeled as molecular switches that tightly fold (“off”) to prevent self-killing in the

Michael Normantovich and Arie Amitzur contributed equally to this work.

This is an open access article under the terms of the [Creative Commons Attribution-NonCommercial-NoDerivs](https://creativecommons.org/licenses/by-nc-nd/4.0/) License, which permits use and distribution in any medium, provided the original work is properly cited, the use is non-commercial and no modifications or adaptations are made.

© 2024 The Authors. *Plant Direct* published by American Society of Plant Biologists and the Society for Experimental Biology and John Wiley & Sons Ltd.

absence of ligand. Effector sensing, often by the LRR domain, causes exchange of ADP for ATP in the NBS domain and activates the protein. The amino-terminal portion usually encodes a TIR (toll/interleukin-1 receptor) domain in the TNL subfamily of NLR proteins, or coiled coil domains (in the CNL subfamily), that evoke downstream signaling (Innes, 2004; Lapin et al., 2022; Ngou et al., 2022; Takken et al., 2006). The recent solving of NLR protein structures greatly advanced our knowledge about their action and signaling through formation of resistosome complexes (Ma et al., 2020; Martin et al., 2020). Pathogen effectors may directly bind the R protein, or alternatively, the R protein may sense perturbation of a specific host protein (the “guardee”) that represents a target of the pathogen effector (Chisholm et al., 2006; van der Hoorn et al., 2008), or a decoy that mimics the guardee and alerts to the presence of an effector. Characterized fungal Avr determinants include proteases, protease inhibitors, chitin binding proteins, toxins, and small secreted proteins of unknown biochemical functions (Koeck et al., 2011; Toruño et al., 2016). With respect to viruses, many viral proteins, including coat proteins, movement proteins, replicases, and proteases were shown to act as Avr factors and be recognized by R-proteins in specific pathosystems (Rouxel & Balescent, 2010).

It is increasingly apparent that R-genes do not act alone. R-Avr interaction involves R-protein oligomerization, assembly with interacting proteins, including “helper NLR” (Jubic et al., 2019), and dynamic re-localization between the nucleus and cytosol (Shen et al., 2007; Slotweg et al., 2010). At the genomic organization level, R-genes mostly reside in clusters where reorganization and transposition events facilitate the evolution of novel specificities (Borrelli et al., 2018; Frantzeskakis et al., 2020). A particular case of specialized evolution that has attracted much attention recently involves pairs of NLR genes residing in a head-to-head orientation (Narusaka et al., 2009). Two well studied R-gene pairs are *RRS1-RPS4* in Arabidopsis, consisting of two TIR-NLR genes, and *RGA4-RGA5* in rice, of the CC-NLR subfamily (Cesari et al., 2014; Williams et al., 2014). *Pik1* and *Pik2* form another rice gene pair (De la Concepcion et al., 2018). In these cases, the two adjacent genes have evolved a “labor division” mode, in which one of the genes acts as a sensor, and the second as an executor NLR. The two proteins are co-expressed and physically interact via their amino-terminal domains. In the absence of the pathogen effector, the sensor protein inhibits signaling by the executor. Upon binding of the effector, inhibition is released and signaling is initiated. The sensor proteins in these two systems have acquired a non-canonical domain (a WRKY domain in the case of *RRS1*, HMA/RATX1 domain in the case of *RGA5* and *Pik1*) that directly binds the Avr factor. Such inserted domains are found in 10% of NLR-homologous sequences, and they often correspond to fragments of defense-related genes already known as guardees of R-proteins (Sarris et al., 2016). Such properties of R-pairs have led to the formulation of the “Integrated Decoy” model (Cesari et al., 2014).

Fusarium oxysporum is a widespread, soil borne fungus, considered to be one of the “Top 10 fungal pathogens in molecular plant pathology” (Dean et al., 2012; Di Pietro et al., 2003). In tomato, NLR-encoding R-genes have been described that react to specific *Fusarium*

f. sp. *lycopersicii* races in a gene-for-gene fashion (Houterman et al., 2007, 2009; Rep et al., 2004). The downstream defense response elicited by different plants following infection by *F. oxysporum* has been studied extensively (e.g., Bai et al., 2013; Berrocal-Lobo & Molina, 2008; Chang et al., 2021; Houterman et al., 2007). Melon pathogenic strains belong to *F. oxysporum* f. sp. *melonis* (FOM). Four pathoraces of FOM, namely FOM 0, FOM 1, FOM 2, and FOM 1.2, were classified based on differential melon genotypes (Risser et al., 1976). Resistance to races 0 and 1 is conferred by the *Fom-2* gene, and resistance to races 0 and 2 by *Fom-1*. The two genes, which provide a durable resistance, were genetically mapped, and DNA markers for breeding were developed (Brotman et al., 2002, 2005; Oumouloud et al., 2008; Périn et al., 2002; Teixeira & Camargo, 2006; Tezuka et al., 2009). Resistance to race 1.2 is controlled by multiple recessive genes (Ficcadenti et al., 2002; Herman & Perl-Treves, 2007; Perchepped et al., 2005).

Papaya ringspot virus (PRSV) belongs to the genus *Potyvirus* that represents the largest, most widespread, and economically important genus of plant RNA viruses (Revers & Garcia, 2015; Shukla et al., 1994). PRSV strains were divided into two biotypes: PRSV-W naturally infects cucurbits but not papaya and PRSV-P infects papaya, and is seldom found in cucurbits (Olarte-Castillo et al., 2011; Tripathi et al., 2008). PRSV-W induces mosaic and stunting symptoms, leaf distortion, and fruit blistering on susceptible melon plants. PRSV particles are flexuous filaments that contain a single-stranded RNA genome of positive polarity. The ~10 kb genome encodes a polyprotein that is processed into 11 mature proteins by three viral-encoded proteases (Urcuqui-Inchima et al., 2001; Vijayapalani et al., 2012). Interactions between potyvirus proteins and between these and host proteins were studied in several systems using different methods (Gao et al., 2012; Haikonen et al., 2013; Xiong & Wang, 2013), and an initial interaction map has been portrayed (Elena & Rodrigo, 2012).

Prv is a dominant R-gene with two distinct alleles for resistance to PRSV. Melon accession PI 414723 carries the *Prv*² allele that reacts to PRSV by systemic necrotic lesions, whereas WMR29 that carries *Prv*¹ remains symptomless (Pitrat & Lecoq, 1983). *Prv* mapped to linkage group IX in the melon genetic map (Périn et al., 2002), tightly linked to *Fom-1*. The cultivars resistant to PRSV are susceptible to FOM race 2, and breeding attempts to bring together the superior *Prv*¹ allele and the *Fom-1* allele have failed. We conducted a long-term effort to map and positionally clone a single candidate for each of the two genes (Brotman et al., 2013) and found that they both encode TIR-NLR proteins within a cluster of R-gene homologs. The *Fom-1* gene, MELO3C022146, was found in close proximity to *Prv*, MELO3C022145, in a head-to-head orientation, their respective start codons being separated by 1.3 kb. In a recent study (Nizan et al., 2023), *Prv* was knocked out and proved to be essential for PRSV resistance. We still do not know whether *Prv* and *Fom-1* act cooperatively, but interestingly, *Prv* has an extra NBS domain at its carboxy-terminus, which could function as an integrated decoy.

In the present study, we investigated the *Prv-Fom-1* gene pair of melon. We explored their expression patterns in resistant and susceptible genotypes using real-time quantitative polymerase chain reaction



(qPCR) and promoter–reporter transcriptional fusions. In order for two R-proteins to interact as a gene pair, they must be co-expressed. Data on expression of such pairs are still scant, and we present detailed evidence of such co-expression at the transcript and promoter activity levels. We also report protein–protein interactions between the Prv resistance protein and the PRSV cylindrical inclusion (CI) protein, which may represent the corresponding ligand. Taken together, these data are consistent with the hypothesis that *Fom-1* and *Prv* may act cooperatively to confer resistance; however, proof of physical and functional interaction between *Prv* and *Fom-1* will require additional studies.

2 | MATERIALS AND METHODS

2.1 | Plant material

Melon plants were germinated in pots, in sterile soil/perlite (3:1) mix, and grown at 26°C, 16:8 h light:dark photoperiod in growth chambers. Table S1 summarizes the genotypes used in this study and their resistance reaction towards four races of *Fusarium oxysporum* f. sp. *melonis* and the potyvirus PRSV.

Inoculation with PRSV was performed by bombardment of cotyledon-stage seedlings with tungsten particles coated with an infective PRSV isolate E2 clone (Desbiez et al., 2012), using a hand-gun device developed and assembled by Gal-On et al. (1997). To confirm effective inoculation, 5–10 seedlings per genotype were left intact and inspected for symptoms of PRSV infection of the susceptible genotype at 15–21 dpi.

Inoculation with *F. oxysporum* f. sp. *melonis* (FOM) race 2 (Kfar Manda strain, kindly provided by Dr. Roni Cohen, ARO, Israel) was according to Brotman et al. (2013). Five to 10 seedlings per genotype were kept after tissue sampling and inspected for wilting and necrosis symptoms of the susceptible genotype, in order to confirm successful inoculation.

2.2 | Plant DNA and RNA extraction, real-time qRT-PCR

For genomic DNA extraction from leaf tissue, we used the protocol described by Rogers and Bendich (1985). RNA was prepared from 50 mg of frozen melon roots or hypocotyl tissue using the RiboEx (GeneAll, cat. no 301-902) or Tri-Reagent protocols (Sigma-Aldrich, USA). First-strand cDNA was synthesized with random primers using qScript Flex cDNA Kit (Quanta). PCRs were carried out in the Fast Real-Time PCR System, Applied Biosystems, Singapore. Each 10 µL reaction mixture contained 2 µL each of 10 nM forward and reverse primers, 5 µL of SYBR Green mix (Applied Biosystems), and 1 µL of 10× diluted cDNA, and standard cycling conditions were applied. Each qPCR experiment was conducted in biological triplicates consisting of three different RNA samples and three technical replicates. To standardize relative transcript quantity (RQ) between samples, the L2

ribosomal protein housekeeping gene was used (Sestili et al., 2014). The primers used for qPCR are given in Table S2.

2.3 | Promoter–reporter gene constructs and GUS staining

The putative promoter sequence of 1303 bp was amplified from genomic DNA of the WMR29 genotype using primers shown in Table S2. Restriction sites for *Bam*HI and *Sal*I were added and used to clone the amplified fragment in two opposite orientations into the pCAMBIA 2300 plant vector upstream of the GUS reporter. For GUS histochemical staining (Jefferson et al., 1987), samples were immersed in GUS staining solution composed of 50 mM PO₄ buffer, pH = 7; 1 mM K-ferricyanide; 1 mM K-ferrocyanide; 1 mM EDTA (pH = 8); 25% methanol, .5% Triton X100, and .05 mg/mL of X-gluc (from a 2.5 mg/mL stock dissolved in dimethyl sulphoxide [DMSO]). Samples were subjected to vacuum for 5 min and incubated overnight in the dark at 37°C. Histological observations were performed using a Leica M205 Stereoscope equipped with a .5× objective and a DFC-7000 dual-mode camera, and driven by LasX acquisition software and a Leica LMD7 wide field upright microscope using the LasX acquisition software.

2.4 | *Agrobacterium rhizogenes* transformation

We generated composite plants by *A. rhizogenes* transformation, using strain K599. To transform bacteria with binary constructs, a starter culture was grown in 5 mL Luria Broth (LB) overnight at 28°C, gently shaken at 180 rpm, re-inoculated to 50 mL of fresh LB medium, and grown to .5 OD₆₀₀. The culture was chilled on ice for 10 min and centrifuged at 3000g for 10 min. The pellet was re-suspended in 2 mL of 2 mM CaCl₂, divided on ice to 100 µL aliquots, and snap-frozen in liquid nitrogen. The cells were thawed on ice; 1 µg of plasmid DNA was added and incubated on ice for 5 min, followed by heat-shock for 25 min at 37°C. Cells were incubated in 1 mL of LB medium for 3 h at 28–30°C, with gentle shaking, and plated for 2 days at 28–30°C on LB-agar medium with antibiotic selection.

2.5 | Generation of composite plants with transgenic roots

Composite plants with stably transformed roots were prepared according to Collier et al. (2005). *A. rhizogenes* cultures harboring the construct of interest were grown for 2 days at 28°C with orbital shaking, in selective LB medium. The bacteria were centrifuged for 5 min at 5000 rpm and re-suspended in .25X MS medium to .25–.5 OD₆₀₀. Seedlings at the cotyledon stage were clipped at the hypocotyl and inserted in sterile rock-wool cubes of 2–3 cm³, saturated with 4 mL/cube of bacterial suspension. Plates with cubes were left open in the growth chamber with no additional watering in order to induce mild

stress (until plants began to lose turgor pressure). Next, the cubes were saturated with tap water, and placed in plastic trays, covered with clear nylon wrap, and kept in the growth chamber at 26°C. Plants were regularly irrigated with tap water until the emergence of adventitious roots, after which they were removed from the rock-wool cubes and transferred to hydroponic medium (Berezin et al., 2012) in plastic boxes of .5 L, five plants/box. The boxes were ventilated using a standard fish tank air pump.

2.6 | Tobacco transformation

Tobacco leaf disks ~ 1 cm in diameter were sterilized and placed on pre-incubation medium: Murashige–Skoog (MS) salts (Duchefa), 3% sucrose, 2 mg/L NAA, 1 mg/L BAP, and 200 μM acetosyringone. Next, the disks were immersed in *Agrobacterium* suspension for 1 min, blotted on sterile Whatman paper, and transferred back to pre-incubation medium for 48 h in the dark. Next, the explants were transferred to selection-regeneration medium: MS salts, 3% sucrose, .1 mg/L NAA, 1 mg/L BAP, 500 mg/L claforan, and 200 mg/L kanamycin. Explants were sub-cultured every 10–14 days. Regenerating shootlets were transferred to rooting medium: MS salts, 3% sucrose, 500 mg/L claforan, and 200 mg/L kanamycin. Rooted plantlets were gently removed, washed of residual agar in tap water, planted in Jiffy-7 peat “cookies,” and later transplanted into small pots for hardening. Well-developed plantlets were transferred to the greenhouse, tested for transgene presence by PCR, and self-pollinated. Transgenic individuals of the T1 generation were selected by germinating surface sterilized seeds on MS-agar medium supplemented with 100 μg/mL kanamycin and scored for transgene presence using PCR and GUS staining. Five individual plants were studied from each construct by free-hand sections of stems and petioles, followed by GUS activity staining.

2.7 | Yeast two hybrid system

Protein interactions were assayed using the Matchmaker Gold Yeast Two-Hybrid system (Clontech), according to the manufacturer’s protocols. Recombinant plasmids that express the interacting partners were prepared in the pGAD-T7 (prey) and pGBK-T7 (bait) vectors (Clontech) and verified by sequencing. To separately clone the 11 open reading frames encoded by the PRSV genome, we used a PRSV infective clone (strain E2, Desbiez et al., 2012) as template for PCR amplification. Primers (Table S2) included unique restriction sites (*Bam*HI and *Sac*I) for ligation into the pGAD-T7 yeast expression vector (Clontech). The entire Prv resistance gene coding sequence (splice variant C) was cloned from melon WMR29 using melon leaf cDNA as a template and primers shown in Table S2. The same ORF was then divided in four regions that included the four domains, similarly amplified and cloned into pGAD-T7: TIR (amino acids 1–248), NBS1 (249–507), LRR (508–1022), and NBS2 (1023–1243).

Transformation of yeast cells (Y2H-gold strain, Clontech) with a pair of plasmids was according to Gietz et al. (1995). Cells were plated

on double-drop-out (DDO) agar medium, devoid of leucine and tryptophan, to select for double transformants, and incubated 2 d at 28°C. Two colonies were isolated from each treatment and grown overnight in liquid DDO complemented with 2% glucose. A tenfold dilution series of the cultures was spotted on triple drop-out medium devoid of leucine, tryptophan, and histidine, the latter reporting on interaction between the bait and the prey. A pair of plasmids encoding two known interactors, p53 and T-antigen, was used as a positive control, whereas the plasmid pair encoding T-antigen and lam provided a negative control.

2.8 | Agroinfiltration and co-immunoprecipitation

Protein coding fragments (NBS2, CI, TIR) were subcloned in-frame with the fluorescent tag proteins, mCherry or GFP. Fragments were amplified by PCR using as templates the plasmids that served for the Y2H assay, primer pairs from Table S2 and Phusion High-Fidelity DNA Polymerase (Thermo Scientific). Fragments underwent blunt-end ligation into the pGEM-T-easy plasmid (Promega), then the desired fragments were released by the designated restriction sites and ligated as in-frame fusions, upstream of the fluorescent tag, into the pNOGA-GFP or the pNOGA-mCherry binary vectors, that consisted of 35S:GFP and 35S:mCherry expression cassettes, respectively, in a pBIN-plus backbone. The two vector plasmids were kindly provided by Dr. Dana Gelbart of the Agricultural Research Organization (ARO), Israel. Following sequence verification, binary plasmids were introduced into *Agrobacterium tumefaciens* EHA105 strain. Leaves of 4-week old *Nicotiana benthamiana* plants were infiltrated with a suspension of the desired *Agrobacterium* strains to transiently express the genes of interest. *Agrobacterium* was cultured at 28°C on a rotatory shaker overnight, in LB supplemented with 100 mg/L rifampicin and 50 mg/L kanamycin. Next, 1 mL of suspension was added to fresh LB + .5 M MES and cultured to a density of $OD_{600} = .5$. The suspension was centrifuged at 4500 rpm for 10 min, resuspended in 10 mL of freshly prepared buffer (10 mM MgCl₂, 10 mM MES, .1 mM acetosyringone), and infiltrated to the abaxial side of leaves, using a needleless syringe. To reduce possible silencing of the inserted genes, plants were infiltrated with a 1:1 ratio mixture of the desired culture with a culture expressing the Tombusvirus silencing suppressor gene, p19 (Lakatos et al., 2004). Three days after agroinfiltration, the infiltrated leaf regions were harvested and ground in liquid nitrogen. Extraction and co-immunoprecipitation was performed according to the GFP-trap manufacturer’s manual (Chromotek). A .5 g tissue sample was ground with .5 mL extraction buffer (10 mM Tris/Cl pH 7.5, 150 mM NaCl, .5 mM EDTA, .5% NP40, 30 μL Protease Inhibitor Cocktail [Sigma], 5 mM dithiothreitol [DTT], and 1 mM phenylmethylsulfonyl fluoride [PMSF]). Samples were centrifuged 5 min at 20,000 g, 4°C, and the tissue pellet was discarded. Centrifugation was repeated three more times to remove any insoluble tissue debris. Protein extracts were diluted by adding 600 μL dilution buffer (10 mM Tris/Cl pH 7.5, 150 mM NaCl, .5 mM EDTA, 30 μL Protease Inhibitor Cocktail [Sigma], and 1 mM PMSF) to 400 μL extract, and 500 μL of the

diluted extract was incubated at 4°C with 25 μ L GFP-trap beads (Chromotek) for 1 h under constant mixing. The supernatant containing non-bound proteins was removed, and the beads were re-suspended in 500 μ L wash buffer (10 mM Tris/Cl pH 7.5, 150 mM NaCl, and .5 mM EDTA) and centrifuged at 4°C, 2500 g for 2 min. Three washes were performed, and the beads were suspended in wash buffer and transferred to a new tube. Bound proteins were eluted with 100 μ L elution buffer (2X sodium dodecyl sulfate [SDS]-sample buffer, consisting of 120 mM Tris/CL PH 6.8, 20% glycerol, 4% SDS, .04% bromophenol blue, and 10% β -mercaptoethanol) for 10 min at 95°C. For Western blot analysis, protein samples were mixed with an equal volume of 2X SDS sample buffer, boiled, and separated on 12% SDS-PAGE electrophoresis gels with Tris-Glycine running buffer. Proteins were transferred to nitrocellulose membranes by electro-blotting, and membranes were incubated with first and secondary antibodies (α -GFP, Biovision; α -mCherry, Abcam; goat α -mouse IgG, Abcam; goat α -rabbit IgG, Jackson) using standard procedures, followed by enhanced chemiluminescence (ECL) detection using an Amersham Imager RGB ImageQuant 680 machine.

3 | RESULTS

3.1 | *Prv* and *Fom-1* undergo alternative splicing

The mRNA transcripts of genes encoding NLRs are often subject to alternative splicing (Lai & Eulgem, 2018). We previously reported two *Prv* splice variants, A and B, that were experimentally confirmed by cloning cDNA molecules that bridge the annotated exons, as well as database cDNA sequences (Brotman et al., 2013). Here we identified three new splice variants, C, D, and E, from additional cDNA clones

from young leaf tissue of melon genotypes WMR29 and Védraçais, which contained complete ORFs of varying length. The five *Prv* variants and their predicted protein sequences are depicted in Figure 1. Exons 1 and 2, which encode the TIR and NBS domains, are identical in all variants. Transcripts A, B, and C contain 2–3 exons encoding LRR regions of varying length and composition, and a C-terminal non-canonical domain, encoding a second NBS region (NBS2). NBS2 is shorter than the first NBS and lacks the conserved RNBS-D and MHD motifs, and therefore, it is unlikely to be a functional nucleotide-binding/hydrolyzing domain. Transcripts D and E represent truncated forms that lack the NBS2 domain, form D terminating with a short LRR region of two LRR motifs, and transcript E possessing no LRR motifs.

We found, by isolating and sequencing melon cDNA molecules from non-inoculated seedling hypocotyl tissue of melon genotypes MR1, WMR29, PI 414723, and Dulce, that *Fom-1* produces two alternative transcripts, A and B (Figure 1b). Both encode the three canonical domains, TIR, NBS, and LRR; however, the product of transcript B lacks the C-terminal part of the TIR domain and the N-terminal portion of the NBS region, including the P-loop, and probably represents an inactive form. DNA alignments of *Prv* and *Fom-1* coding regions in a few melon cultivars are given in Figures S5 and S6, respectively, showing also the primers that were used in the expression studies of the next section below, to selectively amplify the transcripts of different splice variants.

3.2 | Expression of *Prv* and *Fom-1* transcripts

There are only few detailed studies on *R*-gene expression patterns, perhaps because of the typically low transcript levels. Using qRT-PCR,

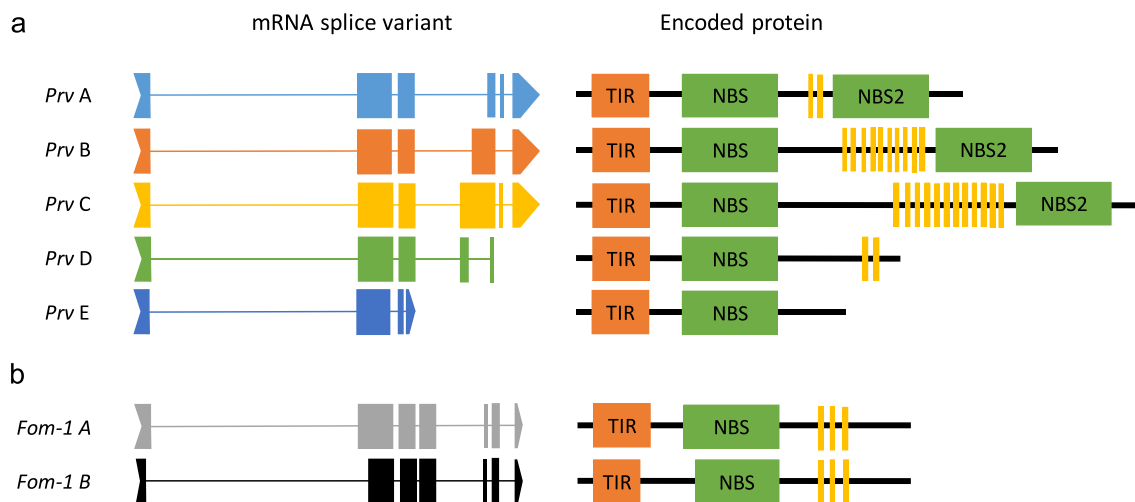


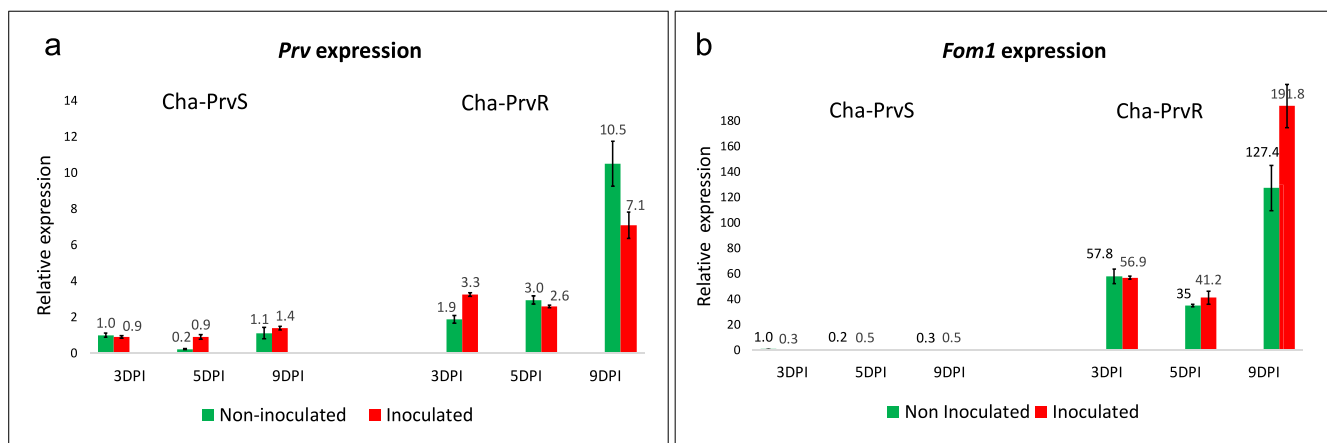
FIGURE 1 Splice variants of the *Prv* (a) and *Fom-1* (b) genes and the respective protein products. Left: gene models showing five splice variants of *Prv* and two of *Fom-1*, drawn to scale with thick bars representing exons and thin lines depicting the introns, between the translation start and stop codons. Right: the corresponding protein domains encoded by each variant. Yellow bars represent LRR repeats. Orange and green boxes represent the TIR region and the nucleotide binding-site-ARC domains, respectively. An updated annotation of these splice variants was submitted under GenBank accession JX295631.

we tested whether expression differed between resistant and susceptible near-isogenic lines, and whether it changed upon pathogen inoculation. In a first experiment, the melon lines Charéntais-PrvR (resistant to PRSV, where the *Prv* locus has been introgressed from melon breeding line WMR29) and Charéntais-PrvS, a susceptible near-isogenic line, were used (Table S1). Seedlings were inoculated with PRSV, and systemic leaves were sampled at 3, 5, and 9 days post-inoculation (dpi), along with similar leaves from non-inoculated seedlings. These time points were selected because they correspond to early through advanced stages of viral spread in susceptible plants. Each sample was mixed from three seedlings, and three separate experiments were run. To quantify *Prv* and *Fom-1* transcripts by qRT-

PCR, we first designed *Prv* variant-specific primer pairs and learned that splice variants A and B are expressed at low to undetectable levels, whereas variants C, D, and E were readily detectable and showed similar patterns of expression (Figure S1A–C). Therefore, a pair of primers that matches all five different splice variants was designed (Table S2) and used for all subsequent analyses.

We observed that the basal transcript levels of *Prv*, in either inoculated or control leaves at all three time points, were twofold to eightfold higher in the resistant isolate, compared to the susceptible isolate (Figure 2a). This trend was apparent in all three replicate experiments (the additional two replicates are shown in Figure S2A, B). We also observed a developmental increase in transcript level from 3 to 9 dpi,

Prv isogenic lines, PRSV inoculation



Fom-1 isogenic lines, FOM2 inoculation

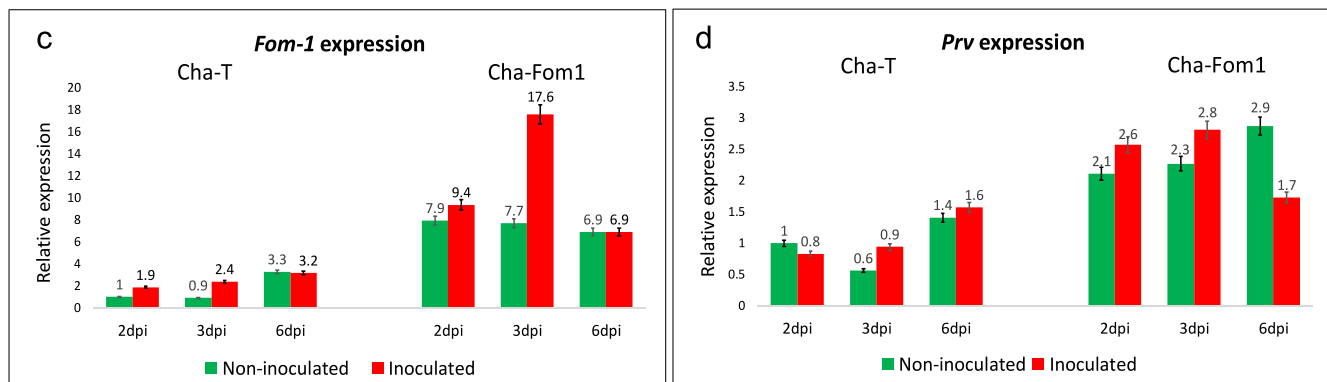


FIGURE 2 Expression of *Prv* and *Fom-1* in melon lines differing in PRSV and FOM2 resistance. Expression of (a) *Prv* and (b) *Fom-1* in a pair of isogenic lines differing in PRSV resistance. Seedlings of Charéntais-PrvR, resistant to PRSV and Charéntais-PrvS, a susceptible isogenic line, were inoculated at the cotyledon stage by particles carrying DNA of a PRSV infective clone, and RNA was prepared from systemic leaves at 3, 5, and 9 dpi, and from non-inoculated samples as a control. Each sample was mixed from three seedlings, and one of three independent replicate experiments is shown. Expression of (c) *FOM-1* and (d) *Prv* in a pair of melon isogenic lines differing in FOM2 resistance. Melon seedlings of Charéntais-Fom1, resistant to FOM races 0 and 2 and Charéntais-T, a susceptible isogenic line, were transferred to hydroponic medium and inoculated with FOM2 spore suspension, and RNA was prepared from roots at 2, 3 and 6 dpi, and from non-inoculated samples as control. Each sample was mixed from five seedlings, and one of two independent replicate experiments is shown. RT-qPCR was performed and relative quantity of transcripts was calculated using the constitutively expressed L2 gene as a standard. RQ values are shown above columns. Bars represent standard errors.

but we did not see consistent induction or repression of *Prv* expression in response to viral inoculation. To confirm the elicitation of a defense response by our inoculation treatment, we also quantified the expression of two defense-related genes, *Dicer-like 4 (DCL4)* involved in anti-viral RNA silencing and *Pathogenesis-related 1 (PR1)* involved in salicylic acid-mediated defenses against various pathogens (Figure S1D, E). We noted a 2.5-fold induction of *DCL4* and a fourfold induction of *PR1* in the resistant line at 5 dpi, and a slower and less conspicuous induction in the susceptible line.

We quantified expression of the neighboring *Fom-1* gene in the same set of samples. In the first experiments, we assayed the expression of splice variants A and B separately. The B variant, which encodes an apparently non-functional protein, was expressed at low levels in the susceptible line and was undetectable in the resistant line (Figure S4A). We therefore assayed variant A in subsequent experiments. Interestingly, we detected a large difference (1–2 orders of magnitude depending on the replicate) between the isolines also for the *Fom-1* transcript (Figure 2b). Like *Prv*, *Fom-1* was not induced by PRSV inoculation; in one replicate, it was even downregulated. The apparent correlation between the expression levels of the *Prv* and *Fom-1* transcripts is further demonstrated by plotting the RQ values in the 18 biological samples (three experiments \times 2 treatments \times 3 time points) from each genotype (Figure S3A), resulting in very high and significant correlation coefficients. This suggests that transcription of these neighboring genes could be co-regulated.

Next, we used another pair of isogenic lines that differ in resistance to FOM races 0 and 2, namely susceptible Charéntais-T and the resistant isoline Charéntais-Fom1 (that obtained the gene from melon cultivar Doublon). Here we sampled roots of hydroponically-grown seedlings that were inoculated with FOM race 2, and non-inoculated seedlings as a control.

We assayed by qRT-PCR the levels of the *Fom-1* and *Prv* transcripts at 2, 3 and 6 dpi. The experiment was repeated twice, yielding similar results, and one of the replicates is shown in Figure 2c, d (for the additional replicate, see Figure S2C). The basal levels of *Fom-1* transcript differ between the two isolines, with twofold to eightfold higher levels in most of the FOM-resistant line samples, compared to the susceptible line samples. In the second replicate, the difference was even larger. In both experiments, at 2 and/or 3 dpi, we observed an approximately twofold increase in *Fom-1* expression upon

inoculation, whereas at 6 dpi, the levels were similar to or lower than the non-inoculated control (Figure 2c). Expression of *Prv* was quantified on the same set of samples. Here again, the levels were, on average, approximately twofold higher in the FOM-resistant line and did not increase upon FOM-2 inoculation in most instances (Figure 2d). In addition, we assayed the transcripts of two known defense genes, *Plant defensin 1.4 (PDF1.4)* and *Peroxidase 34 (PREX34)*. Transcripts of the two marker genes were strongly upregulated (twofold to sevenfold) in the resistant genotype but attained lower levels in the susceptible one (Figure S4B, C).

We plotted the *Prv* and *Fom-1* RQ values across 12 samples of this experiment and, in agreement with our observation in Figure S3A, the values were highly correlated, $R^2 = .71$ and significant (Figure S3B). The correlated levels of basal expression of the two genes suggest that the intergenic sequence could affect their transcription in opposite directions in a similar manner. Nevertheless, pathogen inoculation differentially affects the two genes, suggesting an additional, gene-specific level of regulation.

3.3 | Putative regulatory motifs in the *Fom-1/Prv* intergenic region

The two protein-coding sequences of *Fom-1* and *Prv* in genotype WMR29 (BAC clone JX295631.1) are separated by 1303 bp (Figure 3), and they are transcribed in opposite directions. This 1303-bp interval includes the putative promoter sequences that direct transcription, as well as 5' untranslated regions (5'UTR) of the respective mRNAs. To map the 5'UTR, we used the NCBI graphic viewer, as well as the Cucurbit Genome Browser (http://www.icugi.org/JBrowse/?data=icugi_data%2Fjson%2Fmelon_v361&loc=chr09%3A764284..772534&tracks=DNA%2Cgenes%2CPRJNA434538-Cm_CK_24h%2CPRJNA434538-Cm_PM_24h%2CPRJNA434538-Cm_CK_48h). The RNA-seq data track of the genome browser, showing the filtered transcript coverage, estimates the likely 5'UTR and transcription start sites (TSS) of each gene. According to their annotation, the 5'UTR of the *Fom-1* gene is about 90-bp long, that of *Prv* is about 538 bp, and the remaining non-transcribed spacer is only 598-bp long (Figure 3).

To identify possible transcription factor binding sites (TFBS), a bioinformatics analysis of the same 1303-bp sequence was performed

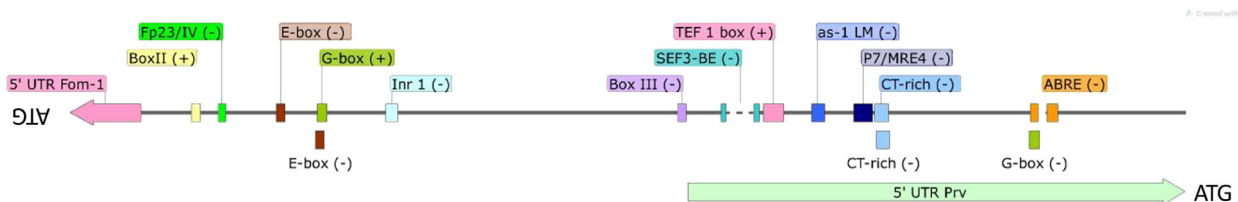


FIGURE 3 Intergenic region of *Fom-1* and *Prv* with putative regulatory motifs. The 1303-bp DNA fragment from melon WMR29 spans the intergenic region between the translation start codons of *Fom-1* on the (–) strand and *Prv* on the (+) strand. Colored arrows show the respective 5'UTR of each gene, based on RNAseq data presented in the melon genome browser by NCBI, as well as the Cucurbit Genome Browser. Colored boxes depict 15 putative transcription regulatory elements detected by the NSITE-PL program (softberry.com). Full detail of these sequence elements is given in Table S3.

using the NSITE-PL program (softberry.com). The analysis detected 15 motifs, consisting of putative TFBS on both strands (Table S3). Motifs shared minimum sequence homology of 80% and statistical significance of .95 to motifs stored in the RegSite Database Plant Regulatory Elements, which contains 3032 entries in total (<http://www.softberry.com/berry.phtml?topic=regsite>).

For seven of the 15 annotated TFBS, the respective transcription factors (TF) have been characterized in the literature. Three of the putative *Fom-1* promoter motifs (i.e., those found on the [-] strand), are hormone related. They include two abscisic acid (ABA) response elements (ABRE), known to bind the AB15 and ABF TF that control the response to ABA (Kimotho et al., 2019; Liu et al., 2013) and a putative E-box element. E-box elements bind RAVL-1 TF that control the expression of the brassinosteroid (BR) receptor, as well as genes responsible for BR production (Je & Han, 2010). The P7/MRE4 motif was shown to bind an *Arabidopsis* transcription factor, GT-4, that plays a role in salt tolerance (Wang et al., 2014). In the *Prv* orientation (+ strand), we identified a putative BoxII element, which is found in a phloem-specific promoter sequence of rice tungro bacilliform virus (RTBV) that binds the RNF2 TF (Yin et al., 1997). Box II and G-Box motifs were recently found in a promoter of a stress-inducible gene, *Zmap*, in maize (Jin et al., 2019). Two G-Box elements are present, one on each strand, whereas all other elements are only detected once.

3.4 | Reporter gene expression driven by the *Fom-1-Prv* intergenic region in melon roots

The spatial expression patterns of *Fom-1* and *Prv* in roots were studied using a promoter-reporter approach. The 1303-bp intergenic sequence, encompassing the 5'UTR and putative promoter, was cloned from the WMR29 genotype into the pCambia2300 binary vector, in two opposite orientations with respect to the GUS reporter gene. This resulted in two binary plasmids, "*Prv* promoter: GUS" and "*Fom-1* promoter: GUS." The Composite Plants method (Collier et al., 2005) was employed to obtain melon plants where part of the root system was stably transformed by *A. rhizogenes* strains carrying the above constructs. For both constructs, about 50% of the adventitious roots that developed expressed GUS activity, confirming that the 1303-bp fragment acted as a functional promoter in both directions.

In roots transformed with *Prv* promoter: GUS, a distinct expression pattern appeared (Figure 4), which starts with strong expression at the root tips of main roots and lateral roots (Figure 4a). The different meristematic tissues are intensively stained, starting from the tip-most regions that include the quiescent zone, protoderm and calyptragen, and the cup-shaped procambium. As the root differentiates, GUS expression concentrates in a tight "sleeve" starting at the vascular tissue differentiation point (Figure 4b). Such "sleeve" probably includes the live xylem parenchymatic cells and perhaps also phloem tissue, seen as files of cells with thick transverse walls (e.g. in Figure 4c, d), that lack the lignified rings or spirals present in the xylem

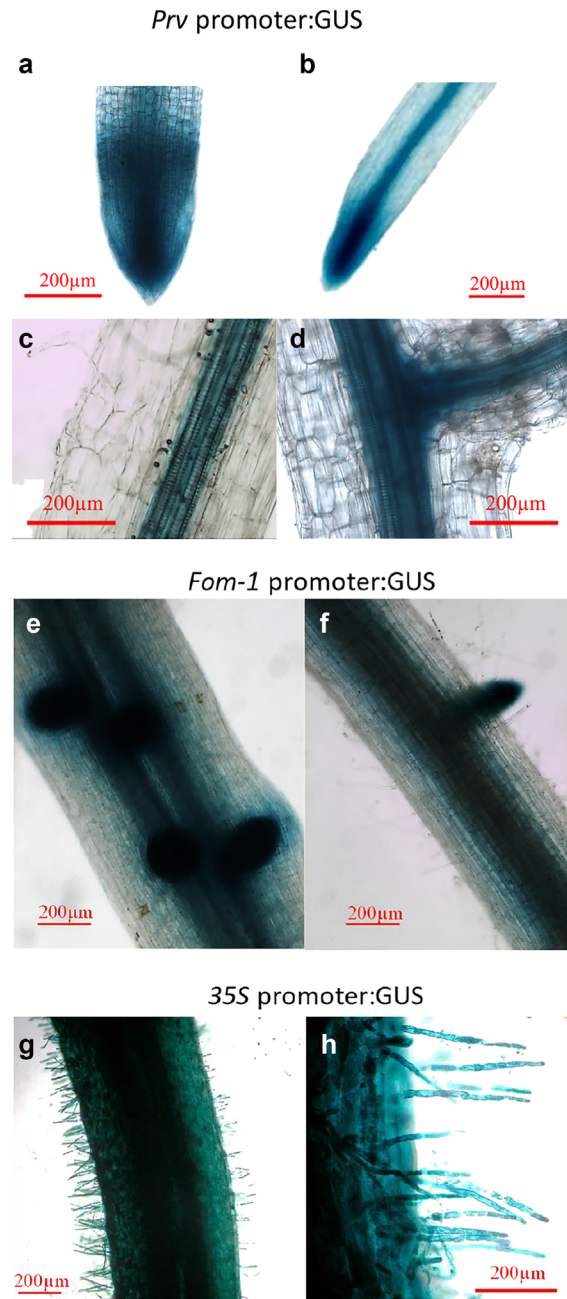


FIGURE 4 GUS activity driven by the *Prv*-*Fom-1* intergenic region in the *Prv* orientation ("*Prv* promoter") and the *Fom-1* orientation ("*Fom-1* promoter") in transgenic melon roots. The 1303-bp intergenic fragment encompassing the 5'UTR and promoter region was cloned upstream the GUS reporter gene, in the two orientations, respectively. The resulting binary vectors were introduced into *Agrobacterium rhizogenes*, and melon seedling hypocotyls were transformed to generate composite plants with stably transformed roots. Whole mount roots were stained for GUS activity. (a-d) Roots expressing the *Prv* promoter: GUS plasmid. (a) Root tip, (b) elongated root, (c) larger magnification of young root, (d) side root branching point. (e, f) Roots expressing the *Fom-1* promoter: GUS plasmid. (g, h) Composite plant roots expressing GUS under the constitutive CaMV 35S promoter. Figure 4a, b, g, h was taken with a Leica M205 stereomicroscope equipped with a .5X objective and a DFC-7000 dual-mode camera, Figure 4c-f with a Leica LMD7 wide field upright microscope using the LasX acquisition software.



vessels; however, the longitudinal live-mount pictures of young roots cannot provide cell-level resolution. In lateral roots (Figure 4d), expression started at the tips and then localized within and around the vascular cylinder. GUS expression was not seen in the root hairs, or the epidermis tissue in general, and was low to absent in the root cortex and root cap, although some variability in expression among samples was apparent.

Roots transformed with the *Fom-1* promoter construct exhibited expression patterns similar to those of *Prv*, with strong GUS expression at the root tips (Figure 4e, f), and little or no expression in the epidermis and root hairs. From the vascular differentiation point upwards, expression was mainly in parenchyma cells surrounding vascular tissue. In some cases, the blue activity zone appeared more diffuse, extending to the cortex tissue, as compared to the tighter expression in *Prv*:GUS roots. With both constructs, strong GUS expression was observed in the lateral roots that emerge from the pericycle and break their way through the cortex, and in the surrounding cortex (Figure 4f). Plants that expressed GUS under the CaMV 35S constitutive promoter exhibited strong expression in all root tissues, including the cortex, epidermis, and root hairs (Figure 4g, h).

3.5 | *Prv*/*Fom-1* promoter analysis in transgenic tobacco plants

After exploring promoter activity in transgenic melon roots, we wished to study expression patterns driven by the *Prv* and *Fom-1* promoters in the shoot as well. Because melon stable transformation is technically difficult, tobacco leaf explants were transformed with the *Prv* and *Fom-1* promoter constructs. T₀ tobacco plants were obtained and self-fertilized in the greenhouse, and five individual T₁ progeny were selected from each construct and studied by free-hand sections of stems and petioles, followed by GUS activity staining.

Although GUS activity varied in intensity among individual plants and according to plant age, several patterns were consistently observed and were similar for both promoter orientations; typical sections are shown in Figure 5a–e and 5f–i for the *Prv* promoter:GUS and *Fom-1* promoter:GUS plants, respectively.

Tobacco stems approaching the flowering stage exhibit a large pith region, apparently devoid of GUS activity (Figure 5a, c), surrounded by bundles of secondary phloem that stain dark blue (Figure 5c, f, g), located on the border between the pith and the xylem vessels. Secondary phloem that forms internally to the xylem is a conspicuous feature of the Solanaceae. In Figure 5b, a leaf is seen emerging from the stem, and GUS activity is located in the axils of the two stipules (leaflet-like appendages) on both sides, in the meristematic zone and in the vasculature of the emerging petiole. In Figure 5c, intensive staining is also apparent in the cambium and primary phloem tissue, and lighter color is also present in the cell files that enlarge and differentiate as xylem vessels, later disappearing as the vessels mature. In some sections and stem region, GUS activity was also detected in the outer part of the cortex, a few cell layers below the epidermis, where smaller and angular collenchyma cells are found; this

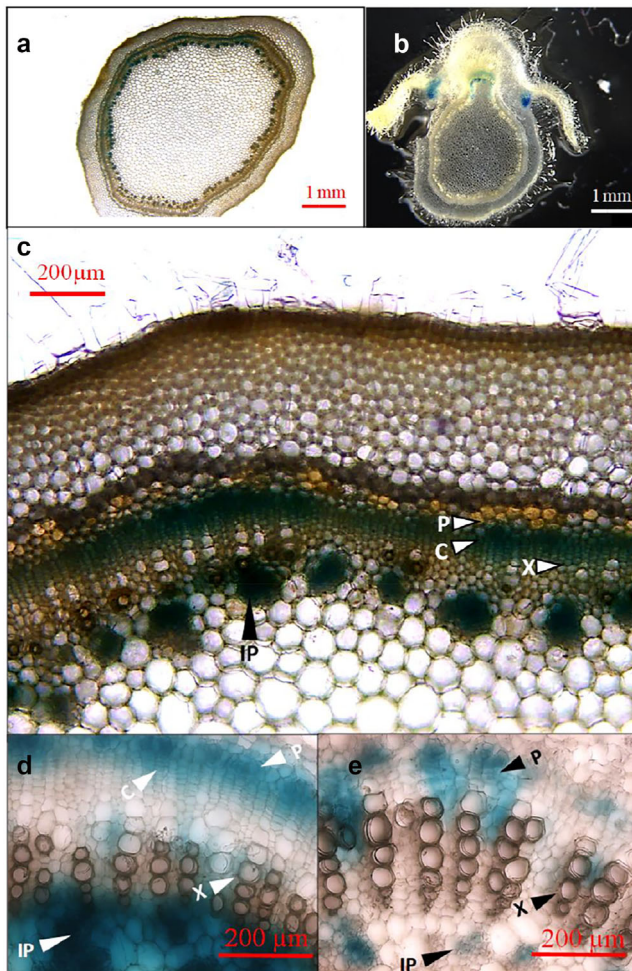
is very conspicuous in the longitudinal section in Figure 5f, where the fainter stain (left side) is the outer cortex/collenchyma; the middle stained region represents the phloem, cambium and younger xylem tissues; and the darkest blue stain is found in the internal phloem. The mature xylem appears brown and lignified and devoid of blue stain; however, a higher magnification section (Figure 5d) shows blue stain in the parenchymatic rays of live cells between the files of differentiating tracheas. The cambium and primary phloem stain as well, and the strongest activity is in the internal phloem and the surrounding parenchyma.

In the tobacco petiole, the major vein appears as a crescent (“smile”) shape (Figure 5h), with the darkest blue stain concentrated in the adaxial (upper surface) phloem, that is derived from the internal phloem of the stem (as seen also in Figure 5b, where the emerging petiole “buds off” the stem vasculature). The Abaxial phloem (towards the lower leaf surface) also stains, as do the parenchymatic cell files between the xylem vessel files. The smaller vascular bundles in the emerging blade on the petiole sides also show strong GUS activity, sometimes extending into the surrounding parenchyma. In the larger magnification of the petiole vascular region taken from a *Prv*:GUS plant (Figure 5e), the phloem, internal phloem, and xylem parenchyma show GUS activity. The activity stain of transgenic tobacco roots (Figure 5i) is similar to that of composite melon roots (Figure 4), with strong activity in root tips and around the vascular cylinder.

3.6 | Interaction between the *Prv* R-protein and a PRSV protein

Resistance proteins of the NLR family recognize pathogen invasion by interacting, either directly or indirectly, with avirulence factors delivered by the pathogen. In a few pairs of *R*-genes, the integrated domain of the sensor protein interacted with a pathogen derived factor. We therefore wished to determine whether one or more proteins encoded by the PRSV genome interact directly with the *Prv* protein. We expressed the entire *Prv* protein of melon WMR29 (splice variant C) as bait in plasmid pGBK-T7, in the yeast two hybrid system (Y2H). We then tested interaction of *Prv* with each of the 11 mature proteins encoded by the PRSV genome expressed as preys in plasmid pGAD-T7. No interactions were observed (Figure S7). We then divided *Prv* into four parts, encompassing the TIR (amino acids 1–248), NBS (aa 249–507), LRR (508–1022), and NBS2 domains (aa 1023–1,243). Each domain was expressed in Y2H as bait with each of the 11 PRSV proteins cloned as prey, resulting in 4 × 11 pairwise combinations. All yeast transformants grew well on media devoid of tryptophan and leucine, showing that the two plasmids were taken up by the yeast strain. However, only the colonies that expressed the C-terminal, non-canonical NBS2 domain together with the PRSV cylindrical inclusion (CI) protein, grew on media devoid of tryptophan, leucine, and histidine (TDO), where histidine auxotrophy reports a likely protein:protein interaction (Figure 6a). The other domains (TIR, NBS1, and LRR) showed no interaction with viral proteins (Figure S7). This result suggests that PRSV may be sensed by the NBS2 “integrated

Prv promoter:GUS



Fom-1 promoter:GUS

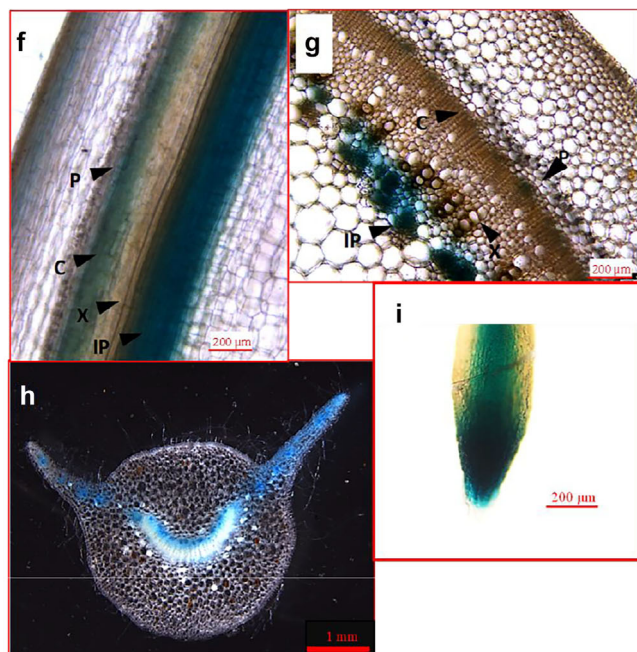


FIGURE 5 The *Prv* promoter:GUS and *Fom-1* promoter:GUS constructs (as in Figure 4) were introduced into *Agrobacterium tumefaciens* and stable transgenic *Nicotiana tabacum* plants were generated. Tissue hand sections from five plants of each construct were stained for GUS activity and observed under the Leica LMD7 wide field upright microscope. (a-e) Plants expressing the *Prv* promoter: GUS plasmid. (a) Cross section in mature stem, (b) cross section in younger stem zone with an emerging leaf petiole, (c) mature stem cross-section, (d) higher magnification of vascular zone in stem cross section, and (e) higher magnification of vascular zone in leaf petiole. (f-i) Plants expressing the *Fom-1* promoter: GUS plasmid. (f) longitudinal section in mature stem, (g) cross section in mature stem, (h) cross section of leaf petiole, and (i) tobacco root tip. In a few of the panels, designated arrows point at X - xylem, P - phloem, IP - internal phloem, and C - cambium.

domain,” that encodes a truncated copy of a nucleotide-binding domain. Among the 11 viral proteins encoded by PRSV, CI represents therefore a candidate for the avirulence factor recognized by the Prv protein in resistant genotypes.

To test whether such interaction occurs also in plant tissues, we applied the agro-infiltration method and expressed tagged versions of CI and NBS2 in *N. benthamiana* leaves. The NBS2 domain of Prv (247 aa; 28 Kd) was tagged with GFP (239 aa; 27 Kd), resulting in a fusion protein of ~55 Kd. The PRSV CI protein (636 aa) was fused to mCherry (237 aa; 28 Kd) resulting in a protein of 98 Kd. In Figure 6b, the “input” samples show that proteins of the expected size were expressed at 3 days after agro-infiltration and detected by the anti-mCherry and anti-GFP antibodies, along with smaller cleavage products that are often seen in such experiments. When we precipitated the NBS-GFP protein with anti-GFP beads, the CI:mCherry protein co-precipitated with it and was eluted from the bound complex (Figure 6b). To exclude that CI:mCherry directly binds the anti-GFP beads, we expressed CI:mCherry alone and saw that it did not precipitate. To exclude that the interaction occurred between the proteins of interest and the GFP or mCherry tags, rather than between CI and NBS2, we co-infiltrated an *Agrobacterium* strain that expresses GFP alone with the CI:mCherry strain, and mCherry alone with NBS2:GFP, and observed no co-precipitation. We concluded that the NBS2:CI interaction detected in yeast also occurs *in vivo* in the plant leaf tissue. However, to prove that such interaction has a role in triggering the defense response, more experiments are needed, for example, mutating CI in the virus, or the NBS2 domain in the plant in a way that will abolish the interaction, to see whether this would render compatible an otherwise incompatible interaction.

4 | DISCUSSION

4.1 | Expression of *Prv* and *Fom-1*

R-genes have been intensively studied in the last decades, but their expression patterns have rarely been analyzed in detail. This study analyzed the expression of mRNA transcripts produced by two melon

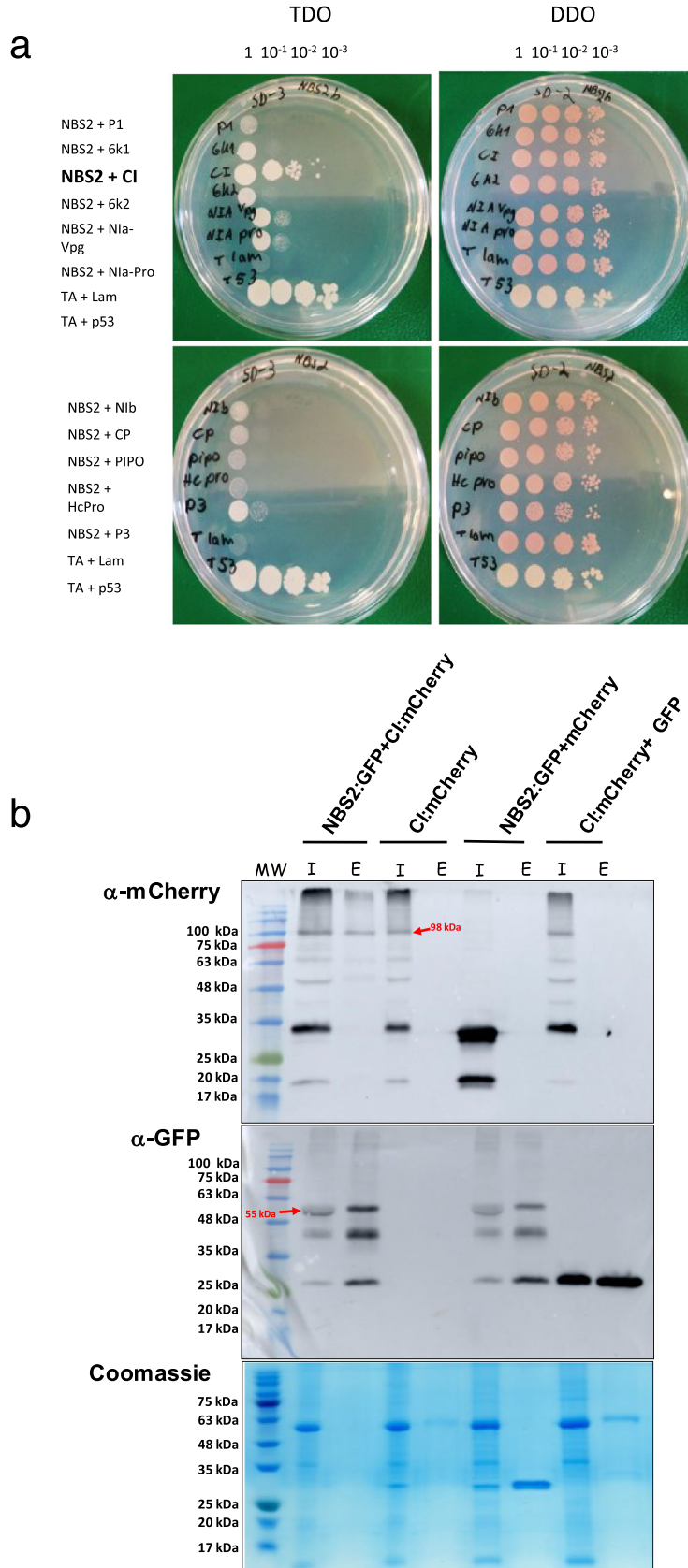


FIGURE 6 Legend on next page.

R-genes, and promoter-reporter constructs that portray the spatial expression patterns of these genes. R-genes are often expressed at a low level, providing plants with constant vigilance against the corresponding pathogen but avoiding the fitness cost involved with unnecessary defense expression. The transcript levels of R genes can be modulated by biotic and abiotic perturbations (MacQueen & Bergelson, 2016), using diverse mechanisms of transcriptional and post transcriptional regulation (Lai & Eulgem, 2018). In some cases, R genes are up-regulated after pathogen attack (e.g., Gu et al., 2005; Rout et al., 2014). For example, the expression of *Xa1*, a rice NLR gene that confers resistance to *Xanthomonas oryzae* pv. *oryzae* in rice, was induced upon inoculation with a bacterial pathogen and by wounding (Yoshimura et al., 1998). The *Rpp4* gene in Arabidopsis is another interesting example that exhibits circadian expression that peaks before dawn, which has likely evolved to anticipate sporulation of the cognate pathogen, *Hyaloperonospora arabidopsidis* (Wang et al., 2011).

In the present study, we identified transcript isoforms of *Prv* and *Fom-1* and followed their expression in response to PRSV or FOM inoculation. We compared pairs of isogenic lines that differed in resistance towards the two pathogens, respectively, encoded by *Prv* and *Fom-1*, and learned that basal expression of *Prv* in the PRSV-resistant line was notably higher than expression in the susceptible isogenic line. In another pair of lines that differed in *Fusarium* resistance, basal expression of *Fom-1* in the FOM resistant genotype was higher than in the susceptible genotype, similar to our observation of *Prv* expression in the PRSV resistant genotype. In both pairs of isogenic lines, the higher basal expression extended also to the neighbor gene. The apparent correlation between the expression levels of the two genes could suggest that the two are expressed in a coordinate manner from the intergenic 1303-bp region that separates them. In such case, TF and *cis*-acting sequence elements enhancing the expression of one gene are also likely to affect the second gene. However, *Fom-1* appears to respond to pathogen inoculation (both to PRSV and *Fusarium*), while *Prv* does not. This could indicate an additional, gene-specific level of regulation acting, perhaps, on top of a shared expression pattern. To learn more about the expression of *Prv* and *Fom-1*, we cloned the 1,303 bp intergenic region in two opposite orientations

upstream the GUS reporter gene. The same DNA fragment drove strong GUS expression in both directions. Interestingly, expression patterns in composite melon roots were very similar in roots transformed with both constructs, mainly concentrating at the root tips and around the root vascular cylinder. A similar pattern of expression was reported by Mes et al. (2000) for the *I-2* gene, that controls *F. oxysporum* resistance in tomato. Moreover, using the same transgenic root system, we investigated the expression of another melon gene, *Fom-2*, that controls resistance to FOM races 0 and 1 (Joobeur et al., 2004), and encodes a non-TIR NLR gene. A 1450-bp DNA fragment upstream the *Fom-2* ORF drove GUS expression around the root vasculature (Normantovich et al., 2012), suggesting that such pattern of expression is consistent with R-protein vigilance of the vascular tissue, to protect against a vascular pathogen such as *F. oxysporum*. While viruses also use the phloem for long-distance movement in plants, the striking similarity of expression pattern driven by the intergenic fragment in both the *Fom-1* and *Prv* orientation suggests that expression of the two genes is coordinated. To extend our observation to the aerial plant parts, we generated tobacco plants that expressed the above *Fom-1* promoter: GUS or *Prv* promoter: GUS constructs. The two reporter gene constructs caused similar expression patterns in stems and petioles, associated with secondary and primary phloem, and also the xylem parenchyma. We note that to demonstrate overlapping spatial expression of the two genes and compare their expression levels more directly, one should express two different reporter genes from the same bi-directional promoter on a single plasmid. Such experimental design was not accomplished in the present study, therefore our correlated expression data remain suggestive.

Eukaryotic promoters upstream of a given gene often support transcription in both directions. “Divergent transcription” in the opposite direction from the gene results in short-lived non-coding RNA that could have regulatory roles (Duttke et al., 2015). Bi-directional promoters, however, control pairs of head-to-head oriented, protein-encoding genes that are transcribed in opposite directions. They represent a significant portion of human genes (~10%, considering pairs less than 1000 bp apart), and correlated expression and function were often observed for the pair members (Wakano et al., 2012). Such

FIGURE 6 Interaction between the cylindrical inclusion protein (CI) of PRSV and the NBS2 domain of the *Prv* resistance protein. (a) Interaction in the yeast two hybrid system between individual PRSV proteins (P1, 6K1, CI, 6K2, NIa-Vpg, NIa-Pro, NIb, CP, PIPO, HC-Pro, P3) cloned as preys in pGAD-T7, and the NBS2 non-canonical domain of the *Prv* protein, cloned as bait in plasmid pGBK-T7. Each row presents serial dilutions of transformed yeast cultures on triple drop-out (TDO) medium that selects for bait-prey interaction (left plate) and double drop-out medium (DDO) that confirms the presence of the two plasmids (right plate). Row TA+53 contains yeast expressing p53 and T-antigen that are known interactors, row marked TA+Lam contains yeast expressing T antigen and Lam as negative control. (b) Co-immunoprecipitation of the *Prv* NBS2 domain with the potyviral CI protein, following their co-expression in *Nicotiana benthamiana* leaves. NBS2 was fused in-frame to GFP, and CI to mCherry. Binary constructs expressing these proteins as well as the mCherry and GFP native proteins were transformed in *Agrobacterium tumefaciens* EHA105 and agro-infiltrated into *N. benthamiana* leaves in various combination as indicated on top of the western blot lanes. For each treatment, we loaded the extract equivalent of ~1 mg leaf fresh weight (I, input). Then we incubated the extract from 120 mg fresh leaf tissue with anti-GFP beads and loaded the eluate of bound proteins (E; derived from ~12 mg tissue extract). Proteins were separated by PAGE on two identical gels, blotted to nitrocellulose, and reacted with anti-mCherry (top panel) and anti-GFP (bottom panel). Red arrows indicate the co-precipitated fusion protein. The bottom panel shows an identical SDS PAGE gel loaded with same amounts of proteins and stained with Coomassie blue, as a loading control. The experiment was repeated three times. MW, molecular weight standard.



genomic organization is considered non-random and ancient. In Arabidopsis, 18% of the genes are organized in divergent pairs compared to 9% in rice and 3% in poplar. They include cases with similar expression patterns of the paired genes, as well as cases of dissimilar expression (Dhadi et al., 2009 and references therein). An interesting example has been reported recently in pepper, where a bi-directional promoter co-regulates a pair of phytoalexin synthesis genes in response to pathogen attack (In et al., 2020). The intergenic region of *Fom-1* and *Prv*, which includes the promoter region and the respective 5' UTR, spans 1303 bp and contains several putative regulatory elements shown, in other plants, to bind known TF. While in certain cases (Dhadi et al., 2009) similar elements were mapped to each strand of a bi-directional promoter, the distribution of such putative motifs in the *Fom-1-Prv* intergenic region is asymmetrical, G-box being the only element found on both strands (Table S3, Figure 3). We still do not know how similar expression patterns are controlled by such a DNA fragment, what are the TF that bind to it, and whether certain motifs can indeed enhance bi-directional expression.

Pairs of head-to-head *R*-genes represent ~10% of the annotated NLR homologs in Arabidopsis (eight pairs out of 174 NLR homologous sequences; Narusaka et al., 2009), and they are of particular interest for understanding *R*-gene evolution. *R*-gene pairs whose protein products interact must be spatially and temporally co-expressed. While the majority of “singleton” *R*-proteins sense the presence of the pathogen, often via the LRR domain, and activate a defense response via their N-terminal CC or TIR domains, paired *R* genes have divided these functions between them. In the few well-studied cases (Cesari et al., 2014; De la Concepcion et al., 2018; Williams et al., 2014), one member, the “sensor”, has acquired an “integrated decoy” domain for sensing the pathogen effector, while losing the ability to generate a downstream response. The second protein, the “executor”, retained the signaling function and remains inhibited by the sensor protein in the absence of the pathogen. Upon binding of the effector, the sensor will relax such inhibition and the executor will activate a response. In two such pairs in rice, *Pik1* and *RGA5* were shown to bind specific effectors of the blast pathogen *Magnaporthe oryzae* via an integrated RATX1/HMA domain (Cesari et al., 2014; Ortiz et al., 2017), while their respective partners, *Pik2* and *RGA4*, act as executors. In a TIR-NLR pair from Arabidopsis, *RRS1* has a WRKY integrated domain that is acetylated by a pathogen effector, leading to activation of an immune response by its partner, *RPS4* (Huh et al., 2017; Le Roux et al., 2015; Williams et al., 2014). It will be interesting to determine whether *Fom-1* and *Prv* in melon act as an *R* gene pair, interacting with each other. The fact that the *Prv* protein possesses a non-canonical domain, consisting of a truncated NBS domain, favors this hypothesis, but direct proof is still required to support the actual function of such domain in *Prv* and a functional interaction of the two neighbor genes in conferring resistance. Sarris et al. (2016) found that, on average, 10% of the NLR genes in plants have extra domains that appear to be enriched for defense-related protein domains. They argued that such “integrated domains” could have arisen from host Avr-targets (“guard-dee” genes) that have been integrated as decoys into *R* proteins. The NBS2 domain of *Prv* is the only case reported of an integrated

nucleotide binding domain, and according to such model, one could speculate that it could have belonged to a helper NLR, acting as a signaling hub in the defense response, becoming a favored Avr target, and eventually being integrated as a decoy in a sensor NLR.

Among the four domains of the *Prv* protein, the only domain that binds a potyviral protein in the Y2H system is the non-canonical NBS2 domain, supporting the interpretation of *Prv* being a sensor protein for PRSV, according to the Integrated Decoy model. NBS2 interacted with the cylindrical inclusion (CI) protein of PRSV, and the Y2H interaction was confirmed by co-immunoprecipitation of the two partners from plant tissue, when CI and NBS2 were transiently expressed in *N. benthamiana* leaves. CI could thus be suggested as a PRSV avirulence factor in resistant melon genotypes, although its actual designation as an Avr factor remains to be proven by functional studies, for example, by mutagenizing CI coding sequence in the virus. CI is a multifunctional potyviral protein that plays roles in replication and generates typical helical bodies in the cytosol that probably act as viral replication factories; it is also involved in viral movement (Sorel et al., 2014). Very few molecular studies exist on potyvirus protein interaction with host *R*-proteins (Kim et al., 2018). In most cases, potyvirus Avr factors have been identified by viral genetics studies, that is, mapping sequence variations/mutations in the virus genome that break resistance. Using such approaches, many different viral proteins were reported to act as Avr factors in different pathosystems, either alone, or together with a second viral protein. For example, Wen et al. (2013) identified the P3 and HcPro proteins of soybean mosaic virus (SMV) as Avr determinants that interact with members of the complex soybean *Rsv1* locus. The CI protein of SMV was also identified as an avirulence determinant (Seo et al., 2009; Zhang et al., 2009). This agrees with our finding that PRSV CI binds directly the *Prv* *R*-protein of melon.

The protein sequences of an *R*-gene pair are expected to reflect their concerted evolution and diversification into sensing and signaling partners, respectively. We aligned the *Prv* coding sequence in five genotypes (Brotman et al., 2013) and reported a very diversified amino acid sequence (average Ka/Ks ratio, i.e., non-synonymous to synonymous substitutions = 1.85). Here, we aligned *Prv* and *Fom-1* primary sequences from three genotypes (Figure S8). We observed lower diversity among 3 *Fom-1* alleles, 14 polymorphic sites/736 residues (1.9%), compared to 39/1193 (3.3%) in *Prv*. This could reasonably indicate that the function of *Fom-1* (the putative executor protein) is more conserved than the function of *Prv* (the putative sensor protein).

According to the model discussed earlier, the executor could be autoactive when expressed alone, while the sensor inhibits the executor but is not required to activate a response by itself, and this could be reflected in their protein sequences. In addition, the pressure on them to co-evolve as a unit and maintain their interaction could render them different from singleton NLRs. We compared the protein sequences of *Fom-1* and *Prv* to those of a few TIR-NLR and CC-NLR to see whether the former proteins could carry inactivating or autoactivating polymorphism. Several studies introduced inactivating and autoactivating point mutations in the NBS and TIR domains of well characterized *R*-genes such as *L6*, *I2*, and *N* (e.g., Bernoux et al., 2011;

Dinesh-Kumar et al., 2000; van Ooijen et al., 2008). When looking at the *Fom-1* and *Prv* sequences, substitutions that correspond to known mutations in highly conserved residues in the TIR and NBS regions could be functionally relevant. Figure S9 displays an alignment of three TIR-NLR protein sequences from other plants (L6, I2, and Mi) with those of *Prv* and *Fom-1*, highlighting residues of proven functional importance. The most studied motif in the ARC2 subdomain of the NBS region is MHD. Substitutions in the invariant histidine and near-invariant aspartate residues often resulted in an autoactive mutant, which is apparently locked in the ATP binding conformation (Bendahmane et al., 2002; Howles et al., 2005). Neither *Prv* nor *Fom-1* harbors a canonical MHD motif. *Prv* has MHI, which is closer to the consensus, whereas *Fom-1* has MPK, which drastically deviates from MHD and could be autoactive. This is similar to the situation in the RGA4 and RGA5 pair, where RGA4 has TYG that probably contributes to its autoactive phenotype. Replacing it with MHD abolished auto activity (Cesari et al., 2014). In the TIR region, many conserved positions, where mutations in known genes resulted in inactivation and susceptibility (and sometimes HR), are conserved in *Fom-1* but not in *Prv*. Examples are residue P160 of L6 (Bernoux et al., 2011) and residues W141 in gene *N* (where S is autoactive; T is found in *Prv*) and R142 (where S is autoactive and found in *Prv*; Dinesh-Kumar et al., 2000). Other apparently critical residues have been changed, relative to consensus, in both *Prv* and *Fom-1*, for example, S161 of L6 (Bernoux et al., 2011), Y12 (when mutated to F it became autoactive, and F is found in both *Prv* and *Fom-1*), and Q67 of *N* (Dinesh-Kumar et al., 2000). However, one should note that the actual outcome of such sequence variation depends on the structural context. It will be important, in future studies, to perform structure–function studies in *Fom-1* and *Prv* in a proper experimental system.

To directly demonstrate functional cooperation between *Prv* and *Fom-1*, we will need to mutate each of them in a suitable genetic background, and see whether mutation in one gene will affect resistance to both FOM and PRSV; this represents a notable challenge in melon. Recently, we have been able to knock-out *Prv* by CRISPR-Cas9 in a PRSV resistant genotype and prove that it is indeed required for PRSV resistance (Nizan et al., 2023); however, functional proof of *Fom-1* function and its possible interaction with *Prv* is still lacking. Another important objective would be to identify the *F. oxysporum* Avr factor recognized by *Fom-1/Prv*. Genetic mapping points at *Fom-1* as encoding a distinct specificity, against *F. oxysporum* races 0 and 2, which appears different from previously described *R*-gene pairs. We still do not know whether this additional specificity can be accommodated with the sensor–executor model, and whether this will hold true in different melon haplotypes. *R* genes that encode multiple resistance traits in the same allele have been described, for example, tomato *Mi*, that confers resistance to root-knot nematodes, potato aphid, whitefly, and psyllid (Casteel et al., 2006). The melon *Vat* allele encodes two traits, aphid resistance and virus transmission by aphids (Dogimont et al., 2014). Other genotypes possess different alleles that encode powdery mildew resistance (Dogimont et al., 2007), and the interesting evolution of alleles and *vat*-like clustered sequences has been studied in depth (Chovelon et al., 2021). The *Rrs1-Rps4* gene pair

in *Arabidopsis* encodes three resistance traits (Narusaka et al., 2009). The pathogen specificities of the *Fom-1-Prv* haplotype, where PRSV resistance and FOM resistance appear to be mutually exclusive and haplotypes that have both resistance alleles were not obtained. Each pathogen specificity could have evolved separately under different pathogen-selection pressures, which shaped both proteins in the gene pair in order to maintain their physical interaction. In such case, swapping single *R*-alleles among haplotypes by genetic recombination would be detrimental.

In conclusion, the present study provides seminal data on the spatial and temporal expression of a pair of *R*-genes, *Fom-1* and *Prv*. Expression is driven by a bidirectional intergenic fragment in opposite directions, resulting in correlated expression patterns. The potential function of *Prv* as a sensor *R* protein in recognition of PRSV was supported by binding of the PRSV CI protein to the non-canonical NBS2 integrated domain of *Prv*. These interesting data are consistent with the hypothesis that *Prv* and *Fom-1* form an integrated decoy pair, and additional experiments are warranted to further investigate their possible interaction.

AUTHOR CONTRIBUTIONS

Michael Normantovich and Arie Amitzur performed a large part of the experiments of this article. Amalia Bar-Ziv, Ekaterina Pashkovsky, Yula Shnaider, Sharon Offri, and Shahar Nizan performed specific experiments. Cécile Desbiez, Christopher G. Taylor, Ohad Yogeve, Avi Jacob and Steven A. Whitham provided specific clones, methods, and know-how for the described experiments. Rafael Perl-Treves planned the project, supervised the students that performed the experiments, and wrote the manuscript. Steven A. Whitham, Shahar Nizan, Arie Amitzur, and Michael Normantovich assisted in reviewing and editing the manuscript.

ACKNOWLEDGMENTS

The authors thank Prof. Simcha Lev-Yadun and Dr. Yoel Melamed for valuable help in interpreting anatomic sections, and Mr. David Levy for growing the plants for the experiments. This research was funded in part by ISF grant No. 16/1137 of the Israel Science Foundation.

CONFLICT OF INTEREST STATEMENT

The Authors did not report any conflict of interest.

PEER REVIEW

The peer review history for this article is available in the supporting information for this article.

DATA AVAILABILITY STATEMENT


All the data of this article is available in the manuscript.

ORCID

Michael Normantovich  <https://orcid.org/0000-0002-5209-1675>

Cécile Desbiez  <https://orcid.org/0000-0001-8691-7423>

Steven A. Whitham  <https://orcid.org/0000-0003-3542-3188>

Rafael Perl-Treves  <https://orcid.org/0000-0003-0294-6900>



REFERENCES

- Bai, T. T., Xie, W. B., Zhou, P. P., Wu, Z. L., Xiao, W. C., Zhou, L., Sun, J., Ruan, X. L., & Li, H. P. (2013). Transcriptome and expression profile analysis of highly resistant and susceptible banana roots challenged with *Fusarium oxysporum* f. sp. *cubense* tropical race 4. *PLoS ONE*, 8, e73945. <https://doi.org/10.1371/journal.pone.0073945>
- Bendahmane, A., Farnham, G., Moffett, P., & Baulcombe, D. C. (2002). Constitutive gain-of-function mutants in a nucleotide binding site-leucine rich repeat protein encoded at the Rx locus of potato. *The Plant Journal*, 32, 195–204. <https://doi.org/10.1046/j.1365-313x.2002.01413.x>
- Berezin, I., Elazar, M., Gaash, R., Avramov-Mor, M., & Shaul, O. (2012). The use of hydroponic growth systems to study the root and shoot ionome of *Arabidopsis thaliana*. In T. Asao (Ed.), *Hydroponics—A standard methodology for plant biological researches* (pp. 135–152). InTech. <https://doi.org/10.5772/36558>
- Bernoux, M., Ve, T., Williams, S., Warren, C., Hatters, D., Valkov, E., Zhang, X., Ellis, J. G., Kobe, B., & Dodds, P. N. (2011). Structural and functional analysis of a plant resistance protein TIR domain reveals interfaces for self-association, signaling, and autoregulation. *Cell Host & Microbe*, 9, 200–211. <https://doi.org/10.1016/j.chom.2011.02.009>
- Berrol-Lobo, M., & Molina, A. (2008). *Arabidopsis* defense response against *Fusarium oxysporum*. *Trends in Plant Science*, 13, 145–150. <https://doi.org/10.1016/j.tplants.2007.12.004>
- Borrelli, G. M., Mazzucotelli, E., Marone, D., Crosatti, C., Michelotti, V., Vale, G., et al. (2018). Regulation and evolution of NLR genes: A close interconnection for plant immunity. *International Journal of Molecular Sciences*, 19, 1662. <https://doi.org/10.3390/ijms19061662>
- Brotman, Y., Kovalski, I., Dogimont, C., Pitrat, C., Portnoy, V., Katzir, N., & Perl-Treves, R. (2005). Molecular markers linked to papaya ring spot-virus resistance and *Fusarium* race-2 resistance in melon. *Theoretical and Applied Genetics*, 110, 337–345.
- Brotman, Y., Normantovich, M., Goldenberg, Z., Zvirin, Z., Kovalski, I., Stovbun, N., Doniger, T., Bolger, A. M., Troadec, C., Bendahmane, A., Cohen, R., Katzir, N., Pitrat, M., Dogimont, C., & Perl-Treves, R. (2013). Dual resistance of melon to *Fusarium oxysporum* races 0 and 2 and to *papaya ringspot virus* is controlled by a pair of head-to-head-oriented NB-LRR genes of unusual architecture. *Molecular Plant*, 6, 235–238. <https://doi.org/10.1093/mp/sss121>
- Brotman, Y., Silberstein, L., Kovalski, I., Périn, C., Dogimont, C., Pitrat, M., Klingler, J., Thompson, G. A., & Perl-Treves, R. (2002). Resistance gene homologues in melon are linked to genetic loci conferring disease and pest resistance. *Theoretical and Applied Genetics*, 104, 1055–1063. <https://doi.org/10.1007/s00122-001-0808-x>
- Casteel, C. L., Walling, L. L., & Paine, T. D. (2006). Behavior and biology of the tomato psyllid, *Bactericera cockerelli*, in response to the Mi-1.2 gene. *Entomologia Experimentalis et Applicata*, 121(1), 67–72. <https://doi.org/10.1111/j.1570-8703.2006.00458.x>
- Cesari, S., Bernoux, M., Moncuquet, P., Kroj, T., & Dodds, P. (2014). A novel conserved mechanism for plant NLR protein pairs: The ‘integrated decoy’ hypothesis. *Frontiers in Plant Science*, 5, 606. <https://doi.org/10.3389/fpls.2014.00606>
- Cesari, S., Kanzaki, H., Fujiwara, T., Bernoux, M., Chalvon, V., Kawano, Y., et al. (2014). The NB-LRR proteins RGA4 and RGA5 interact functionally and physically to confer disease resistance. *The EMBO Journal*, 33, 1941–1959. <https://doi.org/10.15252/embj.201487923>
- Chang, Y., Sun, F., Sun, S., Wang, L., Wu, J., & Zhu, Z. (2021). Transcriptome analysis of resistance to *Fusarium* wilt in mung bean (*Vigna radiata* L.). *Frontiers in Plant Science*, 12, 679629. <https://doi.org/10.3389/fpls.2021.679629>
- Chisholm, S. T., Coaker, G., Day, B., & Staskawicz, B. J. (2006). Host-microbe interactions: Shaping the evolution of the plant immune response. *Cell*, 124, 803–814. <https://doi.org/10.1016/j.cell.2006.02.008>
- Chovelon, V., Feriche-Linares, R., Barreau, G., Chadoeuf, J., Callot, C., Gautier, V., Le Paslier, M.-C., Berad, A., Faivre-Rampant, P., Lagnel, J., & Boissot, N. (2021). Building a cluster of NLR genes conferring resistance to pests and pathogens: The story of the Vat gene cluster in cucurbits. *Horticulture Research*, 8, 72. <https://doi.org/10.1038/s41438-021-00507-0>
- Collier, R., Fuchs, B., Walter, N., Kevin Lutke, W., & Taylor, C. G. (2005). Ex vitro composite plants: An inexpensive, rapid method for root biology. *The Plant Journal*, 43, 449–457. <https://doi.org/10.1111/j.1365-313x.2005.02454.x>
- De la Concepcion, J. C., Franceschetti, M., Maqbool, A., Saitoh, H., Terauchi, R., Kamoun, S., et al. (2018). Polymorphic residues in rice NLRs expand binding and response to effectors of the blast pathogen. *Nature Plants*, 4, 576–585. <https://doi.org/10.1038/s41477-018-0194-x>
- Dean, R., van Kan, J. A. L., Pretorius, Z. A., Hammond-Kosack, K. E., di Pietro, A., Spanu, P. D., et al. (2012). The top 10 fungal pathogens in molecular plant pathology. *Molecular Plant Pathology*, 13, 414–430. <https://doi.org/10.1111/j.1364-3703.2011.00783.x>
- Desbiez, C., Chandeysson, C., Lecoq, H., & Moury, B. (2012). A simple, rapid and efficient way to obtain infectious clones of potyviruses. *Journal of Virological Methods*, 183, 94–97. <https://doi.org/10.1016/j.jviromet.2012.03.035>
- Dhadi, S. R., Krom, N., & Ramakrishna, W. (2009). Genome-wide comparative analysis of putative bidirectional promoters from rice, *Arabidopsis* and *Populus*. *Gene*, 429, 65–73. <https://doi.org/10.1016/j.gene.2008.09.034>
- Di Pietro, A., Madrid, M. P., Caracuel, Z., Delgado-Jarana, J., & Roncero, M. I. (2003). *Fusarium oxysporum*: Exploring the molecular arsenal of a vascular wilt fungus. *Molecular Plant Pathology*, 4, 315–325. <https://doi.org/10.1046/j.1364-3703.2003.00180.x>
- Dinesh-Kumar, S. P., Tham, W. H., & Baker, B. J. (2000). Structure-function analysis of the tobacco mosaic virus resistance gene N. *Proceedings. National Academy of Sciences. United States of America*, 97, 14789–14794. <https://doi.org/10.1073/pnas.97.26.14789>
- Dogimont, C., Chovelon, V., Pauquet, J., Boualem, A., & Bendahmane, A. (2014). The Vat locus encodes for a CC-NBS-LRR protein that confers resistance to a phis gossypii infestation and A. Gossypii-mediated virus resistance. *The Plant Journal*, 80(6), 993–1004. <https://doi.org/10.1111/tpj.12690>
- Dogimont, C., Chovelon, V., Tual, S., Boissot, N., Rittener, V., Giovinazzo, N., & Bendahmane, A. A. (2007). Molecular determinants of recognition specificity at the aphid and powdery mildew Vat/Pm-W resistance locus in melon. In *XIII International congress on molecular plant-microbe interactions*.
- Duttke, S. H., Lacadie, S. A., Ibrahim, M. M., Glass, C. K., Corcoran, D. L., Benner, C., et al. (2015). Human promoters are intrinsically directional. *Molecular Cell*, 57, 674–684. <https://doi.org/10.1016/j.molcel.2014.12.029>
- Elena, S. F., & Rodrigo, G. (2012). Towards an integrated molecular model of plant-virus interactions. *Current Opinion in Virology*, 2, 719–724. <https://doi.org/10.1016/j.coviro.2012.09.004>
- Ficcadenti, N., Sestili, S., Annibaldi, S., Campanelli, G., Belisario, A., Maccaroni, M., & Corazza, L. (2002). Resistance to *Fusarium oxysporum* f.sp. *melonis* race 1.2 in muskmelon lines Nad-1 and Nad-2. *Plant Disease*, 86, 897–900. <https://doi.org/10.1094/PDIS.2002.86.8.897>
- Frantzeskakis, L., di Pietro, A., Rep, M., Schirawski, J., Wu, C.-H., & Panstruga, R. (2020). Rapid evolution in plant-microbe interactions—A molecular genomics perspective. *The New Phytologist*, 225, 1134–1142. <https://doi.org/10.1111/nph.15966>
- Gal-On, A., Meiri, E., Elman, C., Gray, D. J., & Gaba, V. (1997). Simple handheld devices for the efficient infection of plants with viral-encoding constructs by particle bombardment. *Journal of Virological Methods*, 64, 103–110. [https://doi.org/10.1016/S0166-0934\(96\)02146-5](https://doi.org/10.1016/S0166-0934(96)02146-5)

- Gao, R., Tian, Y., Wang, J., Yin, X., Li, X., & Valkonen, J. P. (2012). Construction of an infectious cDNA clone and gene expression vector of tobacco vein banding mosaic virus (genus Potyvirus). *Virus Research*, 169, 276–281. <https://doi.org/10.1016/j.virusres.2012.07.010>
- Gietz, R. D., Schiestl, R. H., Willems, A. R., & Woods, R. A. (1995). Studies on the transformation of intact yeast cells by the LiAc/SS-DNA/PEG procedure. *Yeast*, 11, 355–360. <https://doi.org/10.1002/yea.320110408>
- Gu, K. Y., Yang, B., Tian, D. S., Wu, L. F., Wang, D. J., Sreekala, C., et al. (2005). R gene expression induced by a type-III effector triggers disease resistance in rice. *Nature*, 435, 1122–1125. <https://doi.org/10.1038/nature03630>
- Haikonen, T., Rajamäki, M. L., & Valkonen, J. P. (2013). Interaction of the microtubule-associated host protein HIP2 with viral helper component proteinase is important in infection with Potato virus A. *Molecular Plant-Microbe Interactions*, 26, 734–744. <https://doi.org/10.1094/MPMI-01-13-00>
- Herman, R., & Perl-Treves, R. (2007). Characterization and inheritance of a new source of resistance to *Fusarium oxysporum* f. sp. melonis race 1.2 in Cucumis melo. *Plant Disease*, 91, 1180–1186. <https://doi.org/10.1094/PDIS-91-9-1180>
- Houterman, P. M., Ma, L., Van Ooijen, G., De Vroomen, M. J., Cornelissen, B. J. C., Takken, F. L. W., et al. (2009). The effector protein Avr2 of the xylem-colonizing fungus *Fusarium oxysporum* activates the tomato resistance protein I-2 intracellularly. *The Plant Journal*, 58, 970–978. <https://doi.org/10.1111/j.1365-313X.2009.03838.x>
- Houterman, P. M., Speijer, D., Dekker, H. L., De Koster, C. G., Cornelissen, B. J. C., & Rep, M. (2007). The mixed xylem sap proteome of *Fusarium oxysporum*-infected tomato plants: Short communication. *Molecular Plant Pathology*, 8, 215–221. <https://doi.org/10.1111/j.1364-3703.2007.00384.x>
- Howles, P., Lawrence, G., Finnegan, J., McFadden, H., Ayliffe, M., Dodds, P., & Ellis, J. (2005). Autoactive alleles of the flax L6 rust resistance gene induce non-race-specific rust resistance associated with the hypersensitive response. *Molecular Plant-Microbe Interactions*, 18, 570–582. <https://doi.org/10.1094/MPMI-18-0570>
- Huh, S. U., Cevik, V., Ding, P., Duxbury, Z., Ma, Y., Tomlinson, L., Sarris, P. F., & Jones, J. D. G. (2017). Protein-protein interactions in the RPS4/RRS1 immune receptor complex. *PLoS Pathogens*, 13, e1006376. <https://doi.org/10.1371/journal.ppat.1006376>
- In, S., Lee, H. A., Woo, J., Park, E., & Choi, D. (2020). Molecular characterization of a pathogen-inducible bidirectional promoter from hot pepper (*Capsicum annuum*). *Molecular Plant-Microbe Interactions*, 33, 1330–1339. <https://doi.org/10.1094/MPMI-07-20-0183-R>
- Innes, R. W. (2004). Guarding the goods: New insights into the central alarm system of plants. *Plant Physiology*, 135, 695–701. <https://doi.org/10.1104/pp.104.040410.1>
- Je, B. I., & Han, C. D. (2010). Brassinosteroid homeostasis via coordinate regulation of signaling and synthetic pathways. *Plant Signaling & Behavior*, 5, 1440–1441. <https://doi.org/10.4161/psb.5.11.13357>
- Jefferson, R. A., Kavanagh, T. A., & Bevan, M. W. (1987). GUS fusions: β -glucuronidase as a sensitive and versatile gene fusion marker in higher plants. *The EMBO Journal*, 6, 3901–3907. <https://doi.org/10.1002/j.1460-2075.1987.tb02730.x>
- Jin, B., Sheng, Z., Muhammad, I., Chen, J., & Yang, H. (2019). Cloning and functional analysis of the promoter of a stress-inducible gene (*Zmap*) in maize. *PLoS ONE*, 14, e0211941. <https://doi.org/10.1371/journal.pone.0211941>
- Joobeur, T., King, J. J., Nolin, S. J., Thomas, C. E., & Dean, R. A. (2004). The fusarium wilt resistance locus FOM-2 of melon contains a single resistance gene with complex features. *The Plant Journal*, 39, 283–297. <https://doi.org/10.1111/j.1365-313X.2004.02134.x>
- Jubic, L. M., Saile, S., Furzer, O. J., El Kasm, F., & Dangl, J. L. (2019). Help wanted: Helper NLRs and plant immune responses. *Current Opinion in Plant Biology*, 50, 82–94. <https://doi.org/10.1016/j.pbi.2019.03.013>
- Kim, S.-B. B., Lee, H.-Y. Y., Choi, E.-H. H., Park, E., Kim, J.-H. H., Moon, K.-B. B., et al. (2018). The coiled-coil and leucine-rich repeat domain of the potyvirus resistance protein Pvr4 has a distinct role in signaling and pathogen recognition. *Molecular Plant-Microbe Interactions*, 31, 906–913. <https://doi.org/10.1094/MPMI-12-17-0313-R>
- Kimotho, R. N., Baillo, E. H., & Zhang, Z. (2019). Transcription factors involved in abiotic stress responses in maize (*Zea mays* L.) and their roles in enhanced productivity in the post genomics era. *PeerJ*, 7, e7211. <https://doi.org/10.7717/peerj.7211>
- Koeck, M., Hardham, A. R., & Dodds, P. N. (2011). The role of effectors of biotrophic and hemibiotrophic fungi in infection. *Cellular Microbiology*, 13, 1849–1857. <https://doi.org/10.1111/j.1462-5822.2011.01665.x>
- Lai, Y., & Eulgem, T. (2018). Transcript-level expression control of plant NLR genes. *Molecular Plant Pathology*, 19, 1267–1281. <https://doi.org/10.1111/mpp.12607>
- Lakatos, L., Szittyá, G., Silhavy, D., & Burgyán, J. (2004). Molecular mechanism of RNA silencing suppression mediated by p19 protein of tombusviruses. *The EMBO Journal*, 23, 876–884. <https://doi.org/10.1038/sj.emboj.7600096>
- Lapin, D., Johandrees, O., Wu, Z., Li, X., & Parker, J. E. (2022). Molecular innovations in plant TIR-based immunity signaling. *Plant Cell*, 34, 1479–1496. <https://doi.org/10.1093/PLCELL/KOAC035>
- Le Roux, C., Huet, G., Jauneau, A., Camborde, L., Trémousaygue, D., Kraut, A., et al. (2015). A receptor pair with an integrated decoy converts pathogen disabling of transcription factors to immunity. *Cell*, 161, 1074–1088. <https://doi.org/10.1016/j.cell.2015.04.025>
- Liu, L., Li, N., Yao, C., Meng, S., & Song, C. (2013). Functional analysis of the ABA-responsive protein family in ABA and stress signal transduction in Arabidopsis. *Chin. Scientific Bulletin*, 58, 3721–3730. <https://doi.org/10.1007/s11434-013-5941-9>
- Ma, S. C., Lapin, D., Liu, L., Sun, Y., Song, W., Zhang, X. X., et al. (2020). Direct pathogen-induced assembly of an NLR immune receptor complex to form a holoenzyme. *Science*, 370, 1184. <https://doi.org/10.1126/science.abe3069>
- MacQueen, A., & Bergelson, J. (2016). Modulation of R-gene expression across environments. *Journal of Experimental Botany*, 67, 2093–2105. <https://doi.org/10.1093/jxb/erv530>
- Martin, R., Qi, T., Zhang, H., Liu, F., King, M., Toth, C., Nogales, E., & Staskawicz, B. J. (2020). Structure of the activated ROQ1 resistance directly recognizing the pathogen effector XopQ. *Science*, 370, eabd9993. <https://doi.org/10.1126/science.abd9993>
- Mes, J. J., van Doorn, A. A., Wijbrandi, J., Simons, G., Cornelissen, B. J. C., & Haring, M. A. (2000). Expression of the *Fusarium* resistance gene I-2 colocalizes with the site of fungal containment. *The Plant Journal*, 23(2), 183–193. <https://doi.org/10.1046/j.1365-313x.2000.00765.x>
- Narusaka, M., Shirasu, K., Noutoshi, Y., Kubo, Y., Shiraishi, T., Iwabuchi, M., & Narusaka, Y. (2009). RRS1 and RPS4 provide a dual resistance-gene system against fungal and bacterial pathogens. *The Plant Journal*, 60, 218–226. <https://doi.org/10.1111/j.1365-313X.2009.03949.x>
- Ngou, B. P. M., Ding, P., & Jones, J. D. G. (2022). Thirty years of resistance: Zig-Zag through the plant immune system. *Plant Cell*, 34, 1447–1478. <https://doi.org/10.1093/plcell/koac041>
- Nizan, S., Amitzur, A., Dahan-Meir, T., Benichou, J. I. C., Bar-Ziv, A., & Perl-Treves, R. (2023). Mutagenesis of the melon Prv gene by CRISPR/Cas9 breaks papaya ringspot virus resistance and generates an autoimmune allele with constitutive defense responses. *Journal of Experimental Botany*, 74, 4579–4596. <https://doi.org/10.1093/jxb/erad156>
- Normantovich, M., Yogev, O., Taylor, C. G., & Perl-Treves, R. (2012). Study of the Fom-2 resistance gene using composite melon plants. In



- Cucurbitaceae* 2012 (pp. 240–246). *Proceedings of the Xth EUCARPIA Meeting on Genetics and Breeding of Cucurbitaceae*, 15–18 October, 2012.
- Olarte-Castillo, X. A., Fermin, G., Tabima, J., Rojas, Y., Tennant, P. F., Fuchs, M., et al. (2011). Phylogeography and molecular epidemiology of papaya ringspot virus. *Virus Research*, 159, 132–140. <https://doi.org/10.1016/j.virusres.2011.04.011>
- Ortiz, D., Guillen, K. D., Cesari, S., Chalvon, V., Gracy, J., Padilla, A., et al. (2017). Recognition of the *Magnaporthe oryzae* effector AVR-Pia by the decoy domain of the rice NLR immune receptor RGA5. *Plant Cell*, 29, 156–168. <https://doi.org/10.1105/tpc.16.00435>
- Oumouloud, A., Arnedo-Andres, M. S., Gonzalez-Torres, R., & Alvarez, J. M. (2008). Development of molecular markers linked to the Fom-1 locus for resistance to *Fusarium* race 2 in melon. *Euphytica*, 164, 347–356. <https://doi.org/10.1007/s10681-008-9664-y>
- Perchepped, L., Dogimont, C., & Pitrat, M. (2005). Strain-specific and recessive QTLs involved in the control of partial resistance to *Fusarium oxysporum* f. sp. melonis race 1.2 in a recombinant inbred line population of melon. *Theoretical and Applied Genetics*, 111, 65–74. <https://doi.org/10.1007/s00122-005-1991-y>
- Périn, C., Hagen, L., De Conto, V., Katzir, N., Danin-Poleg, Y., Portnoy, V., et al. (2002). A reference map of *Cucumis melo* based on two recombinant inbred line populations. *Theoretical and Applied Genetics*, 104, 1017–1034. <https://doi.org/10.1007/s00122-002-0864-x>
- Pitrat, M., & Lecoq, H. (1983). Two alleles for watermelon mosaic virus 1 resistance in muskmelon. *Cucurbit Genet. Coop. Rep.*, 6, 52–53.
- Rep, M., Van Der Does, H. C., Meijer, M., Van Wijk, R., Houterman, P. M., Dekker, H. L., et al. (2004). A small, cysteine-rich protein secreted by *Fusarium oxysporum* during colonization of xylem vessels is required for I-3-mediated resistance in tomato. *Molecular Microbiology*, 53, 1373–1383. <https://doi.org/10.1111/j.1365-2958.2004.04177.x>
- Revers, F., & Garcia, J. A. (2015). Molecular biology of *Potyriviruses*. *Advances in Virus Research*, 92, 101–199. <https://doi.org/10.1016/bs.aivir.2014.11.006>
- Risser, G., Banihashemi, Z., & Davis, D. W. (1976). Proposed nomenclature of *Fusarium oxysporum* f.sp. *melonis* races and resistance genes in *Cucumis melo*. *Phytopathology*, 66(9), 1105–1106. <https://doi.org/10.1094/Phyto-66-1105>
- Rogers, S. O., & Bendich, A. J. (1985). Extraction of DNA from milligram amounts of fresh, herbarium and mummified plant tissues. *Plant Molecular Biology*, 5, 69–76. <https://doi.org/10.1007/BF00020088>
- Rout, E., Nanda, S., Nayak, S., & Joshi, R. K. (2014). Molecular characterization of NBS encoding resistance genes and induction analysis of a putative candidate gene linked to *Fusarium* basal rot resistance in *Allium sativum*. *Physiological and Molecular Plant Pathology*, 85, 15–24. <https://doi.org/10.1016/j.pmp.2013.11.003>
- Rouxel, T., & Balescent, M.-H. (2010). Avirulence genes. In eLS. John Wiley & Sons. <https://doi.org/10.1002/9780470015902.a0021267>
- Sarris, P. F., Cevik, V., Dagdas, G., Jones, J. D. G., & Krasileva, K. V. (2016). Comparative analysis of plant immune receptor architectures uncovers host proteins likely targeted by pathogens. *BMC Biology*, 14(1), 8. <https://doi.org/10.1186/s12915-016-0228-7>
- Seo, J.-K., Lee, S.-H., & Kim, K.-H. (2009). Strain-specific cylindrical inclusion protein of soybean mosaic virus elicits extreme resistance and a lethal systemic hypersensitive response in two resistant soybean cultivars. *Molecular Plant-Microbe Interactions*, 22, 1151–1159. <https://doi.org/10.1094/MPMI-22-9-1151>
- Sestili, S., Sebastiani, M. S., Belisario, A., & Ficcadenti, N. (2014). Reference gene selection for gene expression analysis in melon infected by *Fusarium oxysporum* f. sp. *melonis*. *Journal of Plant Biochemistry and Biotechnology*, 23, 238–248. <https://doi.org/10.1007/s13562-013-0207-9>
- Shen, Q. H., Saijo, Y., Mauch, S., Biskup, C., Bieri, S., Keller, B., et al. (2007). Nuclear activity of MLA immune receptors links isolate-specific and basal disease-resistance responses. *Science*, 315, 1098–1103. <https://doi.org/10.1126/science.1136372>
- Shukla, D. D., Ward, C. W., & Brunt, A. A. (1994). *The potyviridae*. CAB International.
- Slootweg, E., Roosien, J., Spiridon, L. N., Petrescu, A.-J., Tameling, W., Joosten, M., Pomp, R., van Schaik, C., Dees, R., Borst, J. W., Smant, G., Schots, A., Bakker, J., & Govers, A. (2010). Nucleocytoplasmic distribution is required for activation of resistance by the potato NB-LRR receptor Rx1 and is balanced by its functional domains. *Plant Cell*, 22, 4195–4215. <https://doi.org/10.1105/tpc.110.077537>
- Sorel, M., Garcia, J. A., & German-Retana, S. (2014). The Potyviridae cylindrical inclusion helicase: A key multipartner and multifunctional protein. *Molecular Plant-Microbe Interactions*, 27, 215–226. <https://doi.org/10.1094/MPMI-11-13-0333-CR>
- Takken, F. L. W., Albrecht, M., & Tameling, W. I. L. (2006). Resistance proteins: Molecular switches of plant defence. *Current Opinion in Plant Biology*, 9, 383–390. <https://doi.org/10.1016/j.pbi.2006.05.009>
- Teixeira, A. P. M., & Camargo, L. E. A. (2006). A molecular marker linked to the Prv1 gene that confers resistance to papaya ringspot virus-type W in melon. *Plant Breeding*, 125(2), 187–190. <https://doi.org/10.1111/j.1439-0523.2006.01198.x>
- Tezuka, T., Waki, K., Yashiro, K., Kuzuya, M., Ishikawa, T., Takatsu, Y., & Miyagi, M. (2009). Construction of a linkage map and identification of DNA markers linked to Fom-1, a gene conferring resistance to *Fusarium oxysporum* f. sp. *melonis* race 2 in melon. *Euphytica*, 168(2), 177–188. <https://doi.org/10.1007/s10681-009-9881-z>
- Toruño, T. Y., Stergiopoulos, I., & Coaker, G. (2016). Plant-pathogen effectors: Cellular probes interfering with plant defenses in spatial and temporal manners. *Annual Review of Phytopathology*, 54, 419–441. <https://doi.org/10.1146/annurev-phyto-080615-100204>
- Tripathi, S., Suzuki, J. Y., Ferreira, S. A., & Gonsalves, D. (2008). *Papaya ringspot virus-P*: Characteristics, pathogenicity, sequence variability and control. *Molecular Plant Pathology*, 9, 269–280. <https://doi.org/10.1111/j.1364-3703.2008.00467.x>
- Urcuqui-Inchima, S., Haenni, A. L., & Bernardi, F. (2001). Potyvirus proteins: A wealth of functions. *Virus Research*, 74, 157–175. [https://doi.org/10.1016/S0168-1702\(01\)00220-9](https://doi.org/10.1016/S0168-1702(01)00220-9)
- van der Hoorn, R. A., & Kamoun, S. (2008). From guard to decoy: A new model for perception of plant pathogen effectors. *Plant Cell*, 20, 2009–2017. <https://doi.org/10.1105/tpc.108.060194>
- van Ooijen, G., Mayr, G., Kasiem, M. M., Albrecht, M., Cornelissen, B. J., & Takken, F. L. (2008). Structure-function analysis of the NB-ARC domain of plant disease resistance proteins. *Journal of Experimental Botany*, 59, 1383–1397. <https://doi.org/10.1093/jxb/ern045>
- van Wersch, S., Tian, L., Hoy, R., & Li, X. (2020). Plant NLRs: The whistle-blowers of plant immunity. *Plant Commun.*, 1(1), 100016. <https://doi.org/10.1016/j.xplc.2019.100016>
- Vijayapalani, P., Maeshima, M., Nagasaki-Takekuchi, N., & Miller, W. A. (2012). Interaction of the trans-frame potyvirus protein P3N-PIPO with host protein PCaP1 facilitates potyvirus movement. *PLoS Pathogens*, 8, e1002639. <https://doi.org/10.1371/journal.ppat.1002639>
- Wakano, C., Byun, J. S., Di, L. J., & Gardner, K. (2012). The dual lives of bidirectional promoters. *Biochimica et Biophysica Acta (BBA)-Gene Regulatory Mechanisms*, 1819(7), 688–693. <https://doi.org/10.1016/j.bbarm.2012.02.006>
- Wang, W., Barnaby, J. Y., Tada, Y., Li, H., Tor, M., Caldelari, D., et al. (2011). Timing of plant immune responses by a central circadian regulator. *Nature*, 470, 110–114. <https://doi.org/10.1038/nature09766>
- Wang, X. H., Li, Q. T., Chen, H. W., Zhang, W. K., Ma, B., Chen, S. Y., & Zhang, J. S. (2014). Trihelix transcription factor GT-4 mediates salt tolerance via interaction with TEM2 in Arabidopsis. *BMC Plant Biology*, 14, 339. <https://doi.org/10.1186/s12870-014-0339-7>
- Wen, R. H., Khatibi, B., Ashfield, T., Saghai Maroof, M. A., & Hajimorad, M. R. (2013). The HC-Pro and P3 cistrons of an avirulent

- soybean mosaic virus are recognized by different resistance genes at the complex Rsv1 locus. *Molecular Plant-Microbe Interactions*, 26, 203–215. <https://doi.org/10.1094/MPMI-06-12-0156-R>
- Williams, S. J., Sohn, K. H., Wan, L., Bernoux, M., Sarris, P. F., Segonzac, C., Ve, T., Ma, Y., Saucet, S. B., Ericsson, D. J., Casey, L. W., Lonhienne, T., Winzor, D. J., Zhang, X., Coerd, A., Parker, J. E., Dodds, P. N., Kobe, B., & Jones, J. D. G. (2014). Structural basis for assembly and function of a heterodimeric plant immune receptor. *Science*, 344, 299–303. <https://doi.org/10.1126/science.1247357>
- Xiong, R., & Wang, A. (2013). SCE1, the SUMO-conjugating enzyme in plants that interacts with N1b, the RNA-dependent RNA polymerase of turnip mosaic virus, is required for viral infection. *Journal of Virology*, 87, 4704–4715. <https://doi.org/10.1128/JVI.02828-12>
- Yin, Y., Zhu, Q., Dai, S., Lamb, C., & Beachy, R. N. (1997). RF2a, a bZIP transcriptional activator of the phloem-specific rice tungro bacilliform virus promoter, functions in vascular development. *The EMBO Journal*, 16, 5247–5259. <https://doi.org/10.1093/emboj/16.17.5247>
- Yoshimura, S., Yamanouchi, U., Katayose, Y., Toki, S., Wang, Z. X., Kono, I., Kurata, N., Yano, M., Iwata, N., & Sasaki, T. (1998). Expression of Xa1, a bacterial blight-resistance gene in rice, is induced by bacterial inoculation. *Proceedings. National Academy of Sciences. United States of America*, 95, 1663–1668. <https://doi.org/10.1073/pnas.95.4.1663>
- Zhang, C., Hajimorad, M. R., Eggenberger, A. L., Tsang, S., Whitham, S. A., & Hill, J. H. (2009). Cytoplasmic inclusion cistron of soybean mosaic virus serves as a virulence determinant on Rsv3-genotype soybean and a symptom determinant. *Virology*, 391, 240–248. <https://doi.org/10.1016/j.virol.2009.06.020>

SUPPORTING INFORMATION

Additional supporting information can be found online in the Supporting Information section at the end of this article.

How to cite this article: Normantovich, M., Amitzur, A., Offri, S., Pashkovsky, E., Shnaider, Y., Nizan, S., Yogev, O., Jacob, A., Taylor, C. G., Desbiez, C., Whitham, S. A., Bar-Ziv, A., & Perl-Treves, R. (2024). The melon *Fom-1-Prv* resistance gene pair: Correlated spatial expression and interaction with a viral protein. *Plant Direct*, 8(2), e565. <https://doi.org/10.1002/pld3.565>